PHILOSOPHICAL TRANSACTIONS A

Review

CrossMark
click for updates

Author for correspondence:
W. H. Matthaeus
e-mail: whm@udel.edu

Intermittency, nonlinear dynamics and dissipation in the solar wind and astrophysical plasmas

W. H. Matthaeus[1,2,3], Minping Wan[1], S. Servidio[2], A. Greco[2], K. T. Osman[4], S. Oughton[5] and P. Dmitruk[6]

[1]Department of Physics and Astronomy, University of Delaware, Newark, DE 19716, USA
[2]Dipartimento di Fisica, Università della Calabria, Arcavacata, Rende, Italy
[3]Dipartimento di Fisica e Astronomia, Università di Firenze, Firenze, Italy
[4]Centre for Fusion, Space and Astrophysics, University of Warwick, Coventry CV4 7AL, UK
[5]Department of Mathematics, University of Waikato, Hamilton, New Zealand
[6]Departamento de Fisica, FCEN, Universidad de Buenos Aires, Buenos Aires, Argentina

An overview is given of important properties of spatial and temporal intermittency, including evidence of its appearance in fluids, magnetofluids and plasmas, and its implications for understanding of heliospheric plasmas. Spatial intermittency is generally associated with formation of sharp gradients and coherent structures. The basic physics of structure generation is ideal, but when dissipation is present it is usually concentrated in regions of strong gradients. This essential feature of spatial intermittency in fluids has been shown recently to carry over to the realm of kinetic plasma, where the dissipation function is not known from first principles. Spatial structures produced in intermittent plasma influence dissipation, heating, and transport and acceleration of charged particles. Temporal intermittency can give rise to very long time correlations or a delayed approach to steady-state conditions, and has been associated with inverse cascade or quasi-inverse cascade systems, with possible implications for heliospheric prediction.

THE ROYAL SOCIETY
PUBLISHING

1. Introduction: structure and intermittency in fluids and plasmas

In order to understand well the dynamics and state of a fluid or plasma system, it is necessary to understand the role of fluctuations. Here we mean fluctuations in quantities such as magnetic field, fluid velocity of various species and density, in plasmas of interest, such as the solar corona, interplanetary medium, diffuse interstellar medium and various parts of the magnetosphere. When the interactions among these fluctuations are nonlinear, the phenomenon is properly called turbulence. The issue addressed in this review is the degree to which nonlinearly interacting fluctuations may be expected to give rise to structure in space and in time. A statistical description of structures and intermittency is particularly relevant as fluctuations in a turbulent medium inevitably display complex behaviour suitable for representation as random variables. Adopting this heuristic definition of intermittency in space plasma turbulence, rather than more formal definitions, is advantageous in our approach, as we explain in the following sections. It may be readily demonstrated that structure formation gives rise to numerous physical effects, many of which may be analysed using several types of simulations or models, ranging from magnetohydrodynamics (MHD) to completely kinetic treatments based on the Vlasov equation. Useful insights are gained by comparison of simulation results and statistics with analogous diagnostics in the solar wind. The emphasis here is to understand the physical connections between intermittency and observable consequences such as coronal and solar wind dissipation and heating, particle transport, and space weather prediction. To assist this understanding, we provide an introduction to the physics of intermittency in space plasmas, recognizing the need to extend the usual (non-intermittent) approach based on uniform homogeneous theoretical treatments, or, when fluctuations are treated, the usual approach based mainly on wavenumber spectra. A dynamical account of intermittency and its consequences necessarily goes beyond these standard approaches.

Spatial structure is typically evident (or can be made so) in realizations of turbulence. The concentrations of vorticity revealed by passive tracers embedded in a rapid flow around an obstacle are a good example, and there are numerous others. Collections of such visualizations, worth examining in some detail, are readily found in print and online, e.g. *An album of fluid motion* [1] or *A gallery of fluid motion* [2]. In these images, it is apparent that spatial intermittency associated with structure is seen in many types of flows when they are strongly nonlinear and when the Reynolds number (or other appropriate dimensionless measures) is high enough to permit a wide range of spatial scales to be represented in the dynamics. Examples are not difficult to find, such as in ocean surface flows, atmospheric flows and in astrophysics. Similarly, temporal intermittency is found in many models, including even nonlinear models of physical phenomena that have been reduced to just a few degrees of freedom, e.g. the Duffing oscillator, the Rikitake dynamo and the Lorentz model.

Historically, the notion of intermittency derives from observation of bursty signals observed in turbulent flows, indicative of occasional very strong spatially localized fluctuations, or localized strong gradients. Sometimes one encounters more formal definitions that are tied to specific models. For example, it is not uncommon to hear it stated that a bursty signal must be multi-fractal (see below) to be considered as intermittency. However, it is clear that the term has been used much more broadly. In particular, Novikov ([3], p. 231) gives a useful definition:

> Intermittency is the nonuniform distribution of eddy formations in a stream. The modulus or the square of the vortex field, the energy dissipation velocity or related quantities quadratic in the gradients of velocity and temperature (of the concentration of passive admixture) may serve as indicators.

In the following sections, we review several types of intermittency and their associated structures and effects on observable phenomena. We will avoid mathematical detail or strict formal definitions, although we will refer to simple mathematical models as elements of the conceptual framework. In this way, we seek not only to provide an accessible introduction but also to

emphasize the various ways that intermittency and dynamically generated structure may have significant impact on observed phenomena in space and astrophysical plasmas. Another goal is to emphasize the early results that have been obtained in extending the more classical approach to understanding fluid intermittency into the much less well understood realm of the low-density plasmas of interest. For these systems, the use of fluid concepts is only an approximation, sometimes a rather crude one, and we do not even know the exact form of the dissipation function. Therefore, the study of intermittency in these cases must proceed simultaneously with a study of some of these very basic physical properties of the dynamics.

Recognizing these goals, the presentation begins with hydrodynamic antecedents but focuses on MHD and plasma behaviour relevant to space and astrophysical plasmas such as the solar wind. We will discuss inertial range intermittency, associated in hydrodynamics with loss of self-similarity at smaller scales, and the Kolmogorov refined similarity hypothesis. In the solar wind context, effects on trapping and transport are described. Next we turn to dissipation range intermittency, or, in a plasma, the intermittency that occurs beyond the inertial range. Here the prospects of non-uniform dissipation and heating are of primary importance. Finally we will briefly mention the role of very-large-scale structure in some systems, which can generate noise of very low frequency that influences predictability by producing a variability of turbulence sources, very much along the lines of the variability envisioned in the seminal works on hydrodynamic intermittency [4,5].

2. Basic diagnostics of intermittency in fluids and magnetohydrodynamics

As we are interested in fluctuating quantities in turbulence, an important way to describe a particular random variable q is through its probability distribution function (PDF), defined by

$$\text{PDF}(q)\,dq = \text{probability that the random value lies between } q \text{ and } q + dq, \qquad (2.1)$$

for infinitesimal dq. Intermittency corresponds to 'extreme events', especially at small scales. The moments of the PDF are $\langle q^n \rangle = \int dq q^n \text{PDF}(q)$; central moments are defined as $\langle (q')^n \rangle$ with $q' = q - \langle q \rangle$. When a random variable is structureless and emerges from an additive random process subject to a central limit theorem, then its distribution is expected to be Gaussian. Recall that, for a Gaussian, odd central moments are zero, and all even central moments $\langle (q')^n \rangle$, n even, are fully determined by $\langle (q')^2 \rangle$.

The so-called longitudinal increment of a random velocity field $v(x)$ is a quantity often discussed in turbulence theory, and is defined as

$$\delta v_r(x) = \hat{r} \cdot [v(x + r) - v(x)], \qquad (2.2)$$

where the vector lag r is of magnitude r and in direction $\hat{r}$. Denoting the magnetic field as $b(x)$, we may define its longitudinal increment, δb_r, in a similar way, and the increment of a scalar by analogy.

When the dynamics leads to the presence of structures at a wide range of scales, higher order moments of increments δv_r are expected to show greater non-Gaussianity at small lags r. For intermittency—in which strong gradients are highly localized—one expects that higher order (integer $p > 3$) moments of smaller scale increments, e.g. $\langle |\delta v_r|^p \rangle$, are much greater than their Gaussian values. The quantity $S^{(p)}(r) = \langle \delta v_r^p \rangle$ is called the pth order longitudinal structure function of the velocity $\mathbf{v}$.

One way to measure this phenomenon is to examine the kurtosis of the increments, defined as

$$\kappa(r) = \frac{\langle \delta v_r^4 \rangle}{\langle \delta v_r^2 \rangle^2}. \qquad (2.3)$$

A simple heuristic interpretation of $\kappa(r)$ is that it is related to the filling fraction F for structures at that scale, with $\kappa \sim 1/F$. Thus, if $\kappa(r)$ increases for smaller r, the fraction of volume occupied by structures at scale r is decreasing with decreasing r.
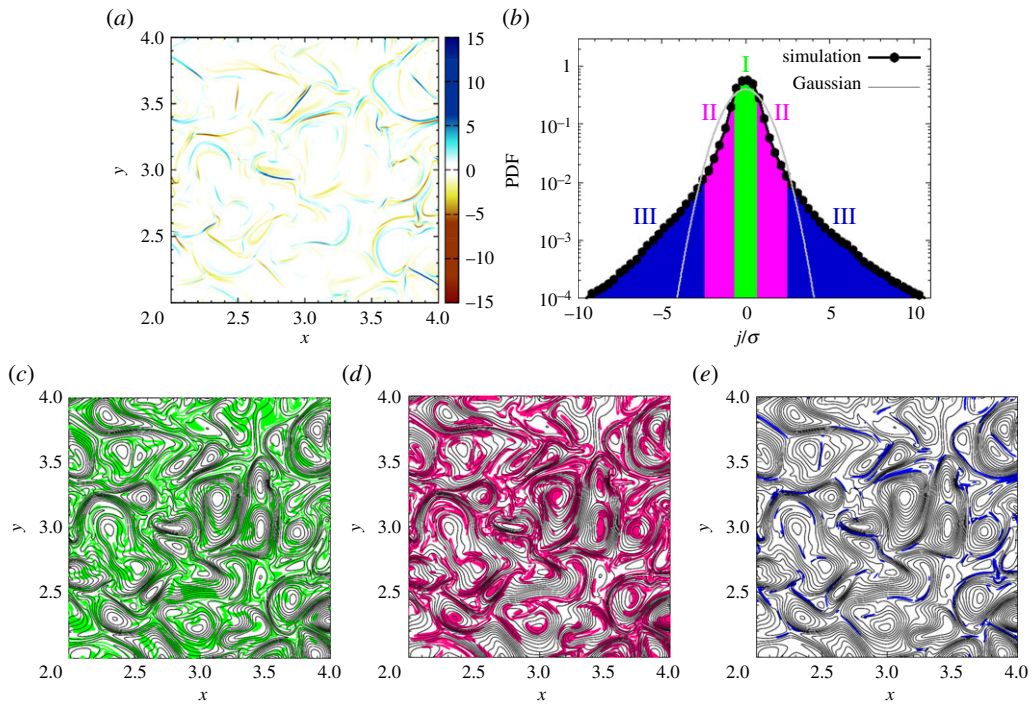
Figure 1. Results from a two-dimensional MHD simulation showing the relationship between the spatial distribution of electric current density (*a*) and various contributions to the PDF of current density (*b*). In both panels, the current density is normalized to its r.m.s. value. The PDF in (*b*) is divided into three regions and is compared with a reference unit variance Gaussian distribution. Region (I), the core of the distribution, corresponds to the shaded regions in (*c*). The sub-Gaussian region designated (II) in (*b*) corresponds to the shaded areas in (*d*). (*e*) The extreme events, i.e. region (III) in (*b*), suggesting that strong current sheets are located between magnetic islands. Magnetic field lines are superposed in (*c*)–(*e*). (Online version in colour.)

The last statement is related to the operating definition of intermittency given by Frisch [6], who states that '... the random function $v(t)$ is intermittent at small scales if the (kurtosis) ... grows without bound with the filter frequency Ω.' Frisch's filtered kurtosis (his 'flatness') is defined in the time domain in analogy to κ but, instead of a spatial increment, it employs a high pass filter at frequency Ω. An example of an intermittent magnetic field in a moderate Reynolds number two-dimensional MHD simulation is shown in figure 1.

The most familiar impact of intermittency in turbulence theory is embodied in the evolution of inertial range theory from Kolmogorov's original (K41) treatment to his 1962 (K62) treatment [5,7]. In the self-similar K41 case [7], the statistics of the inertial increments are determined universally in terms of the dimensionless variable $\delta v_r / (\epsilon r)^{1/3}$, where $\epsilon = \langle \epsilon(x) \rangle$ is the global energy dissipation rate associated with the cascade. Note that transfer from scale to scale is assumed to be local in the scale r. Based on these assumptions, one finds immediately expressions for all moments of the increments:

$$\left\langle \delta v_r^p \right\rangle = C_p \epsilon^{p/3} r^{p/3}. \tag{2.4}$$

The classical K41 case, which treats the hydrodynamic dissipation rate as a constant, has been the motivation for a vast amount of research involving spectra and second-order moments [6,8], as well as closures and phenomenologies of turbulence and turbulent dissipation that have proven useful in many contexts (e.g. [9]).

The K62 theory [5] recognizes that the dissipation function (*local* rate of dissipation: $\epsilon(x)$) is not a uniform constant but rather must be treated as a fluctuating random variable in the same way as the turbulent velocity. The local dissipation coarse-grained to a scale r may be

defined as $\epsilon_r(x) = (\pi r^3/6)^{-1} \int d^3 y \epsilon(x+y)$, where the integration domain is the sphere of radius $r/2$ centred at x. K62 proceeds to adopt the *refined similarity hypothesis*, or KRSH, by introducing a dimensionless random variable $\delta v_r/(\epsilon_r r)^{1/3}$ and arguing that the statistical distribution of this quantity approaches a universal functional form at large values of the Reynolds number. One may again compute moments of the increments to find

$$\left\langle \delta v_r^p \right\rangle = C_p \left\langle \epsilon_r^{p/3} \right\rangle r^{p/3}. \tag{2.5}$$

The effects of intermittency and coherent structures are apparent: unless $\epsilon_r(x)$ is uniform, the exponent $p/3$ will not commute with the averaging operation. In fact, when the medium is intermittent, large increments occur in concentrations in space, where gradients are strong. If these large values occur more frequently than would be expected from Gaussian statistics, then there are 'heavy tails' on the increment distributions. Accepting the similarity hypothesis equation (2.5), it is clear that spatial enhancements of increments are associated with enhancement of the local average dissipation function $\epsilon_r(x)$.[1] Thus, in regions where dissipation is very concentrated over a scale r, there will be concomitant concentration of large values of δv_r. For a given value of average dissipation $\langle \epsilon(x) \rangle = \epsilon$, this effect causes equation (2.4) to differ greatly from equation (2.5), given that $\langle \epsilon_r^{p/3} \rangle \gg \epsilon^{p/3}$ when the intermittency is great. The K62 formulation further makes use of a suggestion by Oboukhov [4] that the exponent $p/3$ may be brought outside the bracket at the expense of adjusting for the concentration of dissipation at the scale r. This replacement introduces a dependence on the outer (energy-containing) scale L, through $\langle \epsilon_r^{p/3} \rangle \rightarrow \epsilon^{p/3}(L/r)^{\xi(p)}$, which indicates an enhancement for $\xi > 0$ associated with the concentration of the dissipation. When the lag approaches the outer scale, $\epsilon_r \rightarrow \epsilon$ and there is no enhancement. With this additional hypothesis, the KRSH postulates that

$$\left\langle \delta v_r^p \right\rangle = C_p' \epsilon^{p/3} r^{p/3 - \xi(p)}, \tag{2.6}$$

where the dimensional factor involving the outer scale is absorbed into the constant C_p'. The quantity $\xi(p)$ is called the *intermittency correction* or sometimes *intermittency parameter*; the combination $\zeta(p) = p/3 - \xi(p)$ is called the *scaling exponent*. When $p = 3$, comparison of equations (2.5) and (2.6) indicates that $\xi(3) = 0$. This is also reminiscent of the exact Kolmogorov third-order law, which, however, involved the *signed* third-order moment. (We have implicitly assumed here that the moments are of $|\delta v_r|$, which appears to be required as $\epsilon_r \geq 0$.)

So far, we have concentrated on hydrodynamic theory although our goal is to discuss MHD and plasma intermittency effects. There is good reason for this. The KRSH for hydrodynamics is the basis for most intermittency theory [10], is considered to be supported by experiments and simulations and is reasonably successful even though not proven. A major derivative effort has been in anomalous scaling theories, including multi-fractal theory [6,11], that are capable of modelling the observed behaviour of higher order structure functions through equation (2.6) and specific functional forms of $\xi(p)$. It is important to understand the status of these theories, which are mainly phenomenological, before extending the ideas to plasmas and MHD.

Like hydrodynamics, MHD theory based on extensions of K41, including uniform constant dissipation rates [12,13], has led to numerous advances, including closures, that have greatly increased understanding of this more complex form of turbulence. However, it is also natural to expect that taking into account the dynamical generation of coherent structures and their effects on dissipation will have rich implications for MHD and plasma, as it does in the transition from K41 to K62 perspectives on hydrodynamics.

The most obvious approach to extending the above ideas to plasmas is to consider the incompressible MHD model in which the velocity increments δv_r and magnetic increments δb_r are treated on equal footing. Without delving more deeply into the background theory, one may

---

[1]The association of enhanced viscous dissipation with enhanced spatial derivatives of velocity requires no hypothesis, as the local rate of viscous dissipation for incompressible hydrodynamics is $\epsilon(x) = (\nu/2) S_{ij} S_{ij}$ with $S_{ij} \equiv \partial_i u_j + \partial_j u_i$.
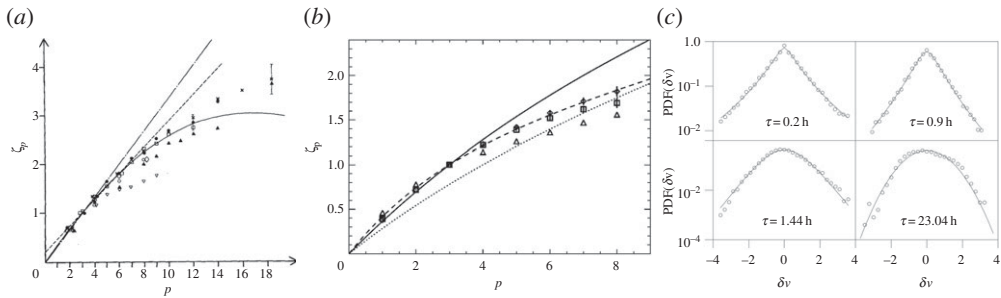
Figure 2. Evidence for intermittency, in the form of multi-fractal scalings of structure functions of increasing order. (*a*) $\zeta(p)$ from hydrodynamic experiments. (Adapted from Anselmet *et al.* [14].) (*b*) $\zeta(p)$ from an MHD simulation. (Adapted from Biskamp & Müller [15].) When the scaling exponent $\zeta(p)$ exhibits anomalous behaviour (i.e. is a nonlinear function of p, the order of the structure function), the scaling is described as multi-fractal [6]. An alternative and more direct approach to characterize intermittency is to compare the PDFs of increments at different spatial lags, finding that fatter non-Gaussian tails appear in the PDFs of the smaller lags. (*c*) An example from solar wind data, where spatial lag is proportional to time lag. (Adapted from Sorriso-Valvo *et al.* [16].)

simply adopt a perspective based on analogy with equation (2.6) and proceed to evaluate higher order statistics and their scalings with spatial lag. From this emerges a picture quite reminiscent of hydrodynamics, as illustrated in figure 2.

Despite what might appear to be an encouraging similarity in the scaling of higher order moments in hydrodynamics and in MHD, there are in fact at least two main impediments to a direct extension of the KRSH to MHD, and at least one additional major problem in extending it to kinetic plasma, as follows.

First, for both MHD and plasma, there is ambiguity regarding the choice of fluid-scale variables as there are now at least two vector fields involved. These are the velocity v and magnetic field b, or equivalently the two Elsasser fields $z^+ = v + b/\sqrt{4\pi\rho}$ and $z^- = v - b/\sqrt{4\pi\rho}$, where ρ is the mass density. (When the magnetic quantities are expressed in Alfvén speed units, the Elsasser variables take the form $z^\pm = v \pm b$.) Is the local dissipation related to δv_r? To δb_r? More properly, based on the structure of the third-order law for MHD [17,18], perhaps relations analogous to equation (2.6) should be written separately for two local dissipation functions ϵ_r^+ and ϵ_r^-, in terms of the increment combinations $(\delta z^+|\delta z^-|^2)^{1/3}$ and $(\delta z^-|\delta z^+|^2)^{1/3}$ [19]. There have also been suggestions that even more information could be embedded in the primitive increment functions entering the MHD KRSH, for example by allowing for a scaling of alignment angles between v and b [20]. All such suggestions are permissible from a dimensional standpoint, but we have not yet seen in the literature either a precise statement of an MHD KRSH (however, see [21,22]) or a full statistical test of any such hypothesis, as has been carried out repeatedly in the hydrodynamic case [23,24].

Second, there is increasing evidence that MHD turbulence lacks a universal character [19,25], so that it is not clear that there is a single, simple answer to the questions posed in the previous paragraph. Non-universality is related not only to the multiplicity of independent field variables in MHD but also to the known sensitivity to parameters that are not related to conserved quantities, such as the Alfvén ratio (ratio of kinetic to magnetic energy) in the initial data or in the driving. One may also see, based on the hierarchy of von Kármán–Howarth-like equations for correlation functions in MHD [19], that the behaviour of the third-order correlations that relate directly to dissipation are themselves dependent upon *several* fourth-order correlations— and not just a single fourth-order correlation as in isotropic hydrodynamic turbulence. These controlling fourth-order correlations, as well as parameters such as the Alfvén ratio, describe the specific turbulence under consideration. Varying these quantities changes the character of MHD turbulence realizations at a significant level [25,26]. These observations provide interesting challenges, but are of course not conclusive. At present, the status of universality in MHD is not

fully established and we may anticipate further work in this area, even as we recognize that MHD turbulence is more complex than its hydrodynamic counterpart.

Finally, in the case of low collisionality or collisionless plasma, there is the additional difficulty that the dissipation function $\epsilon_r(x)$ is not a matter of agreement. Therefore, for the plasma case there are substantial ambiguities, in some sense, on both sides of equation (2.6).

Despite these formal difficulties in extending the mathematical framework of hydrodynamic intermittency to the cases of interest here, in the following sections, we will argue that it is possible to formulate a description of the effects of intermittency in relevant space and astrophysical systems, often with guidance from numerical simulations.

3. Basic physics underlying intermittency

The tendency of nonlinear couplings in a fluid system to produce concentrated spatial structure and non-Gaussianity in higher order statistics can be understood at least partly using simple heuristic ideas, and some simple simulation-based demonstrations.

The amplification of higher order moments by quadratic nonlinearities can be seen as follows. Consider a simple dynamical model in two variables q and w, both functions of space, with the structure $\dot{q} \sim qw$, and initial conditions such that the distributions of q and w begin as Gaussian random variables. Then it is simple to see that the change in q over a short interval Δt is $\Delta q \sim q(0)w(0)\Delta t$, and that this is non-Gaussian. This follows because the product of two Gaussian random variables is a random variable having a kurtosis between 6 and 9, the specific value depending on both the relative variances and the correlation between q and w (e.g. [27]). Thus, we see that the time advancement of a quadratically nonlinear system will progress away from Gaussianity and will probably become less space filling. If we insert a 'wavenumber' k into the equation, so that $\dot{q} \sim kqw$, as in the Fourier space version of an advective nonlinearity, we can similarly conclude that the dynamical variables at smaller scale will become non-Gaussian at a greater rate.

The idea that advection alone can produce concentrations of gradients and statistics similar to intermittency has been applied to devise schemes for generation of synthetic intermittency. The major development in this area has been the minimal Lagrangian mapping method (MLMM) for generating a velocity field that displays numerous characteristics of intermittent turbulence, without running a simulation code to solve the Navier–Stokes or Euler equations [28,29]. The method was recently extended to generation of intermittent magnetic fields [30]. The procedure is based on an iteration in which the velocity field is low-pass filtered at progressively smaller scales, and at each stage the filtered velocity is employed to map the full velocity by approximately one appropriately coarse-grained grid scale. After remapping to the vertices, applying a solenoidal projection, and rescaling the energy spectrum, the procedure is repeated several times. The result is a velocity or magnetic field with a specified spectrum, a realistic scale-dependent kurtosis, and, for the velocity, a negative derivative skewness. Such models may be useful for test particle studies and other applications where a readily available intermittent field is needed, but one also gains some insight in understanding how advection amplifies local gradients and produces intermittency.

These simple heuristic arguments suggest that non-Gaussianity can be produced by *ideal*, i.e. non-dissipative, processes alone. The notion that the small-scale coherent structures seen in observed or computed turbulence are mainly of ideal non-dissipative origin can also be directly tested in numerical simulation. This issue relates directly to the ideal development of the cascade, and indirectly to the question of singularity formation in ideal flows. An early examination of these questions for MHD was given by Frisch *et al.* [31], who studied the formation of sharp current sheets in ideal MHD. The same point was illustrated more recently in two-dimensional MHD simulations [32], by examining higher order statistics such as the filtered kurtosis of the magnetic field. In particular, starting from a single initial condition, the evolution is compared when computed separately in ideal MHD and in viscous resistive MHD at moderately large Reynolds numbers. It is apparent from the results (figure 3) that the current sheets that form
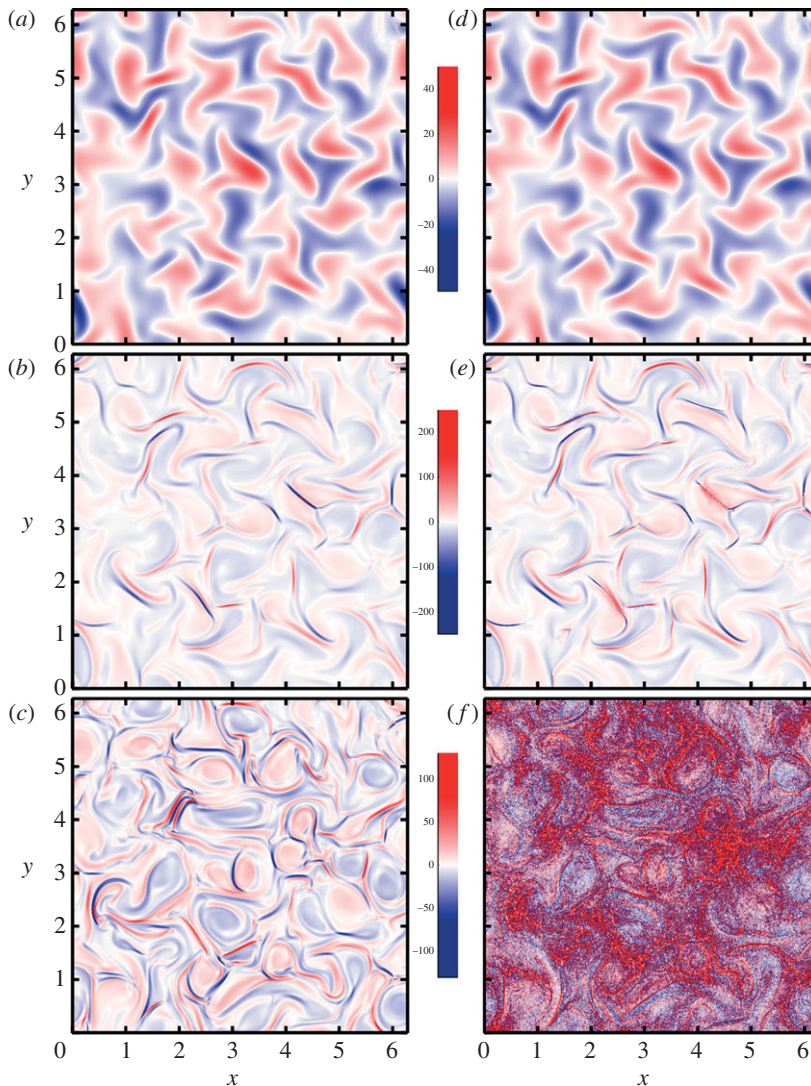
Figure 3. Out-of-plane electric current density from ideal (*a–c*) and resistive (*d–f*) MHD runs started with identical initial data. The current density is shown at three times: $t = 0$, $t \approx 0.2$ nonlinear times and at a later time. The early evolution is evidently almost exactly the same in the two cases. In particular, strong sheet-like concentrations form in both ideal and non-ideal cases. (From Wan *et al.* [32].) (Online version in colour.)

at early times in the ideal case are essentially identical to those formed in the well-resolved dissipative run.

A quantitative comparison of the statistics of the ideal and non-ideal current in the same numerical experiments also reveals that at early times—that is, prior to significant amounts of excitation transferring out to the maximum wavenumber—the kurtosis of the current is essentially the same in the ideal and non-ideal runs.

The close correspondence of the ideal and non-ideal runs up until a time limited by the spatial resolution of the numerics fits well into a cascade picture in which the spectral transfer is ideal and occurs freely and without dissipation throughout an 'inertial range'. When arriving at sufficiently smaller scales, dissipation begins to become important and eventually dominant. This is just the classic K41 perspective. However, the generation of coherent structures in the inertial range of scales, without any apparent influence of dissipation, prompts further reflection. Evidently, the driver of the formation of small-scale coherent structures is found in the ideal nonlinearities.

Dissipation acts mainly to limit the intensification of these coherent structures in space. There is no contradiction of the KRSH implied by this, but rather a subtlety in its interpretation. The stresses that drive structure formation do not involve dissipation, but, when dissipation is computed, its statistical distribution in space measured in the inertial range is a direct response to the statistical distribution of the structures. A simple picture emerges, in which, for large driven systems, it is possible to achieve balance between ideal structure formation and structure deterioration owing to non-ideal effects. In that case one finds a steady transfer through inertial range scales, balanced by intermittent dissipation at small scales.

4. Dynamical relaxation, cellularization and intermittency

The multiplicity of variables, conservation laws and other parameters in incompressible MHD introduces ambiguity in attempts to extend ideas such as the KRSH. The situation is even worse for a kinetic plasma. Multiplicity of variables and parameters also makes it difficult to envision universality in MHD. There are in fact expected to be numerous types of possible turbulent behaviours depending on ratios of ideal invariants, ratios of kinetic to magnetic energies and so on [19,25,26]. On the bright side, this complexity introduces a richness to intermittent MHD turbulence that extends beyond hydrodynamic antecedents.

The role of advection in generation of intermittency seems fairly clear based on the several examples discussed in the prior section. The pile-up of gradients also requires a region of slowdown or diversion so that the transported quantity may be concentrated. For hydrodynamic shear layers, this role is evidently provided at least in part by stagnation points or layers, where vortex amplification into sheets or tubes is likely to occur. For MHD there are more possibilities, as the magnetic field also provides a direction of transport of various quantities, including energy. Therefore, stagnation points of the magnetic field, or neutral points (including component neutral points), occupy a key role in the generation of current sheets, and other coherent structures.

The combined effects of transport and concentration of gradients at special positions leads to important self-organization properties of many fluid systems including MHD, and, as we shall discuss below, also kinetic plasma turbulence. One may effectively argue that these processes at the relatively fast dynamical relaxation times of the system lead to a *cellularization* consisting of relatively relaxed regions separated by strong gradients. The emergence of organized structure is seen in many types of systems, as illustrated in figure 4.

The formation of cellular structure is a clear example of self-organization associated with turbulence, as shall be evidenced in the ensuing discussion. Turbulent relaxation leading to formation of large-scale structure is often associated with important ideas such as Taylor relaxation [38] and selective decay processes [39,40]. Generally, these refer to processes driven by turbulence in which one global quantity (often energy) is preferentially dissipated while another global quantity, or quantities, is maintained at a constant (or near constant) value.[2] One proceeds, for example, by minimizing the incompressible turbulence energy $E = \int d^3x(v^2 + b^2)$ subject to constancy of the magnetic helicity $H_m = \int d^3x\, a \cdot b$, where $b = \nabla \times a$. Applying appropriate boundary conditions and solving the Euler–Lagrange equations corresponding to minimization of E/H_m leads to the so-called Taylor state in reversed field pinch experiments or spheromaks [45].

The corresponding problem for homogeneous turbulence with both cross helicity and magnetic helicity held constant in three dimensions [46] (or, for two dimensions, with mean square potential substituted for H_m [47]) leads to the variational problem $\delta \int d^3x(v^2 + b^2 + \alpha a \cdot b + \gamma v \cdot b) = 0$, and an Euler–Lagrange equation, which has the solution

$$c_1 b = c_2 v = c_3 \nabla \times b = c_4 \nabla \times v. \qquad (4.1)$$

---

[2]Ideal quadratic invariants form the basis of absolute equilibrium models of ideal hydrodynamics and MHD [41–44] which describe how these quantities tend to distribute themselves in the absence of dissipation. While not direct representations of physical systems, these models imply preferred directions of spectral transfer of the conserved quantities, which in turn indicate which quantities might be preferentially dissipated or preserved in real dissipative turbulence.
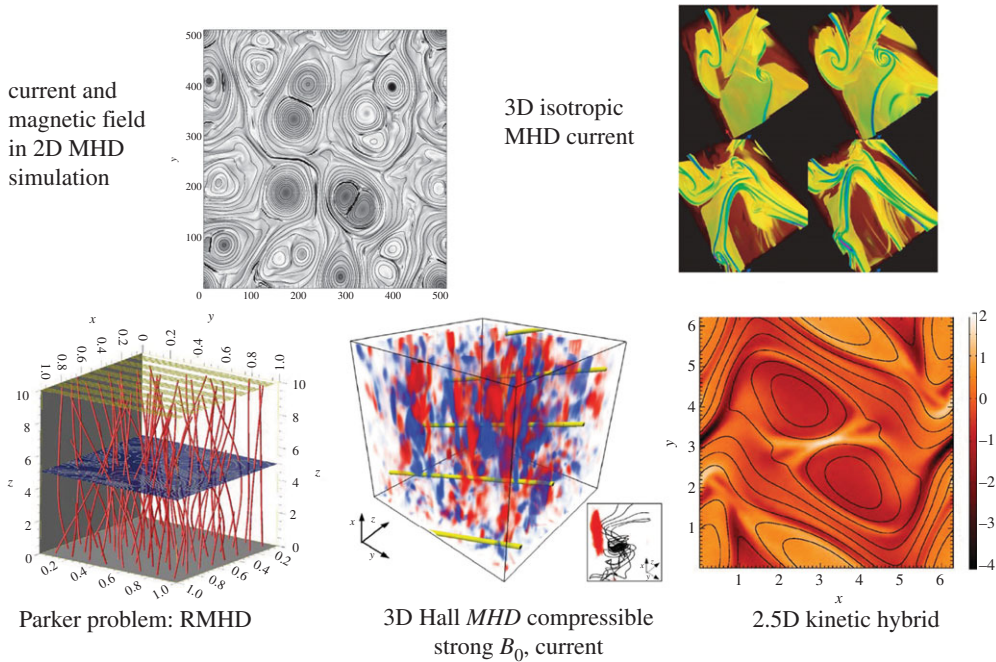
current and magnetic field in 2D MHD simulation

3D isotropic MHD current

Parker problem: RMHD

3D Hall *MHD* compressible strong B_0, current

2.5D kinetic hybrid

Figure 4. Examples of cellularization owing to turbulence—consisting of sharp gradients separating relatively relaxed regions. Shown are turbulence simulation examples from two-dimensional (2D) MHD, three-dimensional (3D) isotropic MHD, reduced MHD (RMHD), 3D Hall MHD and 2.5-dimensional (2.5D) hybrid kinetic codes, respectively, from Zhou *et al.* [33], Mininni *et al.* [34], Rappazzo *et al.* [35], Greco *et al.* [36] and Parashar *et al.* [37]. (Online version in colour.)

The quantities c_1, c_2, c_3 and c_4 are related to the geometry and the Lagrange multipliers α and γ. Note that $\nabla \times \boldsymbol{b} \equiv \boldsymbol{j}$ is the electric current density in MHD, while $\nabla \times \boldsymbol{v} \equiv \boldsymbol{\omega}$ is the vorticity. Equation (4.1) implies that the relaxed state is

$$\text{Alfvénic with } \boldsymbol{v} \propto \boldsymbol{b}, \quad \text{AND} \quad \text{force free with } \boldsymbol{b} \propto \nabla \times \boldsymbol{b}, \quad \text{AND} \quad \text{Beltrami with } \boldsymbol{v} \propto \nabla \times \boldsymbol{v}.$$

In the initial formulations [38–40], the examination of the relaxation processes associated with selective decay focused on the long-time states described by the minimization procedure. In such cases, the Lagrange multipliers and $c_1 \ldots c_4$ are constants that define a global state.

The intermediate states were also discussed, for example, when Taylor [38] describes the temporary conservation of magnetic helicity on each closed flux surface, or when Matthaeus & Montgomery [40] describe the attainment of the final state through successive reconnections between strongly interacting pairs of magnetic flux tubes. It was, however, in the realm of hydrodynamics that the quantitative implications of *local* rapid relaxation processes were described. The local emergence of Beltrami states was found [48–50] to lead to a statistical depression of nonlinearity in turbulence not associated with driving by a dominant large-scale shear flow (in other words, freely relaxing turbulence rather than driven turbulence.) Somewhat later, it was discovered numerically [51,52] (see also [53]) that Alfvénic correlations in MHD turbulence occur spontaneously in patches. Simulation subsequently showed [54] that all three types of correlations—Alfvénic, Beltrami and force free—occur spontaneously, concurrently and rapidly in MHD turbulence. When the relaxation is local, one may anticipate that the physically relevant solutions to equation (4.1) are those with piecewise constant values of $c_1 \ldots c_4$. Additional correlations also emerge, such as anti-correlation of mechanical and thermal pressure. Some of these correlations are shown in figure 5.
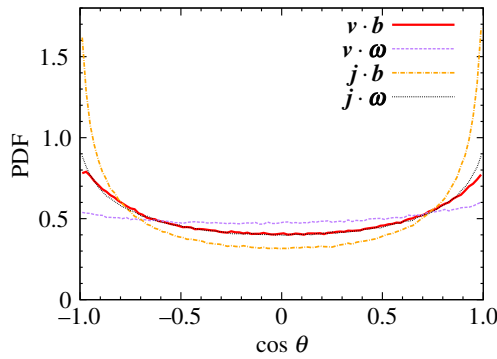
Figure 5. Distributions of the alignment angles between v and b, etc. (see legend), from an unforced three-dimensional MHD turbulence simulation. As in the text, $\nabla \times b = j$ is the electric current density, and $\nabla \times v = \omega$ is the vorticity. The distributions are computed less than one nonlinear time into the run. At $t = 0$ the distributions were all flat. The initial conditions contained very low levels of magnetic helicity and cross helicity. (From Servidio *et al.* [54].) (Online version in colour.)

What all of these emergent correlations have in common is that they decrease the strength of nonlinearities in the equations of motion. Rapid emergence of Alfvénic correlation reduces the strength of the $\nabla \times (v \times b)$ nonlinearity in the induction equation. Similarly, the emergence of local patches of force-free correlation reduces the Lorentz force $(\nabla \times b) \times b$, and patches of Beltrami correlation reduce the strength of $v \times (\nabla \times v)$, and both of these reduce nonlinearity in the momentum equation. It is interesting to note that the appearance of these characteristic correlations in local patches can apparently be made formally compatible with equation (4.1), by allowing the Lagrange multipliers to be piecewise constant, thus enforcing the minimization principle in patch-like regions. A more complete theory based on this idea has yet to be developed as far as we are aware.

This kind of rapid depression (sometimes also called suppression or depletion) of nonlinearity makes good physical sense: in turbulence, fluid elements experience complex forces and accelerations that are difficult to describe in detail. On average, the responses to these forces should act to decrease the forces and acceleration. But on short time scales this effect can occur only locally. Rapid relaxation occurs in cells or patches, with distinct cells relaxing differently. Each region relaxes as far as it can before stresses are built up along boundaries with other relaxing cells. The higher stress boundary regions become concentrated, forming small-scale coherent structures, including vortex sheets and current sheets. These separate relatively relaxed regions, in which the nonlinear stresses are partially depleted. The partially relaxed regions form larger scale 'cells' which are a different sort of coherent structure, such as 'sinh-Poisson' vortices in two-dimensional hydrodynamics [55,56] or flux tubes in MHD.[3]

It is not difficult to show that the emergence of these nonlinearity-suppressing correlations must be associated with non-Gaussian statistics. Intuitively, it is clear as sharp boundaries form between cells and these are non-spacefilling and highly concentrated. This implies non-Gaussianity and high kurtosis of gradients and small-scale increments. This conclusion is also readily verified quantitatively, by evaluation of a fourth-order statistic $H_4 = \langle (v \cdot b)^2 \rangle$, for two special cases. For simplicity, suppose v and b have equal and isotropic variances, and zero mean values, so that the variance of any component is σ^2. For the first case, we assume both vector fields are Gaussian, generated by a jointly normal distribution, and let the the components of b and v be uncorrelated, so that $\langle v_\alpha v_\beta \rangle = 0$ and $\langle b_\alpha b_\beta \rangle = 0$ when $\alpha \neq \beta$, and $\langle v_\alpha b_\beta \rangle = 0$ for all α and β.

---

[3]The concept of entropy that enters the formalism for long time relaxation in two-dimensional hydrodynamics [55] is essentially an information entropy, and must be distinguished from the Gibbs entropy in the absolute equilibrium models [41,43,44]. There have been some attempts to extend the information entropy formulation to *local* two-dimensional hydrodynamic relaxation within individual vortices [57]. Formulations of entropy concepts in MHD have been proposed but are less well studied [39,58].

Then by direct evaluation $H_4 = \langle (\boldsymbol{v} \cdot \boldsymbol{b})^2 \rangle = 3\sigma^4$. As with all jointly normal statistics, the fourth and all higher orders are determined by the first- and second-order moments, including the cross correlation, which here is zero. For the second case, assume that at every point $\boldsymbol{v} = \pm\boldsymbol{b}$, and that the distribution of each may or may not be Gaussian. After a short calculation, one finds for this case that $H_4 = (3\kappa_0 + 6)\sigma^4$, where κ_0 is the kurtosis of any one Cartesian component (all assumed equal by isotropy). In this case, if the fields are Gaussian ($\kappa_0 = 3$), then the assumed pointwise correlation means that H_4 is five times larger than in the fully Gaussian jointly normal case. Thus the joint distribution cannot be normal. For $\kappa_0 > 3$ the disparity is even greater. We conclude that the presence of strong random Alfvénic correlations distributed in patches cannot be described by jointly normal (bivariate Gaussian) statistics, as has been argued previously [52].

One may devise analogous arguments to conclude that each of the local correlations required for depression of nonlinearity requires some level of departure from Gaussianity. That is, correlations such as $\langle (\boldsymbol{b} \cdot \nabla \times \boldsymbol{b})^2 \rangle$ or $\langle (\boldsymbol{v} \cdot \nabla \times \boldsymbol{v})^2 \rangle$ must take on values other than those associated with jointly normal distributions. This has been demonstrated explicitly in three-dimensional MHD turbulence simulations [54] by computing these correlations (and others) from dynamical simulation data, and comparing the values from MHD solutions with values obtained by fixing the spectrum of all quantities and randomizing ('Gaussianizing') the fields $\boldsymbol{v}$ and $\boldsymbol{b}$. This provides a rather convincing quantitative demonstration of the association of depression of nonlinearity with the emergence of non-Gaussianity and intermittency. In these cases, the examination of the real space structure shows patches of relaxed magnetofluid, forming cellularized patterns (e.g. 'flux tubes') that are separated by thin high-stress boundaries, often in the form of current sheets and vortex sheets, as suggested by the examples in figure 4.

The picture that emerges from studies such as those reviewed here is that the turbulent cascade is far from a structureless, self-similar or random-phased collection of fluctuations as is sometimes imagined. Numerical realizations of cascades, as well as observations of turbulence, reveal that nonlinear dynamics leads to local relaxation and the spontaneous creation of regions of reduced nonlinearity, bounded by higher stress concentrations of gradients. This perspective links cascade, relaxation, coherent structures, intermittency and dissipation in a physically appealing picture that is complementary to the more mathematical view of intermittency in terms of anomalous scaling and fractal descriptions. It also makes clear that there is much more to a turbulence description than what is accessible simply by discussion of the power spectrum itself [59].

5. Evidence for coherent structures in the solar wind

Given the accessibility of the solar wind as a natural laboratory for turbulence studies, it is natural to enquire whether the characterization of intermittent turbulence given above is consistent with interplanetary observations.

The most obvious feature of solar wind observations that relates to the picture of cellular flux tube structure of MHD and plasma turbulence is the frequent appearance of discontinuities. These have been studied for decades [60,61], often interpreted as an example of the relevance of simple ideal MHD solutions to the solar wind [60–62]. If, alternatively, the discontinuities are features of turbulence, then a methodology is needed that can compare properties, preferably statistical properties, of discontinuities in a known turbulence environment, such as MHD simulation, with the observed discontinuities in the solar wind. One such approach is the partial variance of increments (PVI) method, which was designed precisely for this purpose [36,63]. The PVI time series is defined in terms of the vector magnetic field increment $\Delta\boldsymbol{B}(s, \tau) = \boldsymbol{B}(s + \tau) - \boldsymbol{B}(s)$, which is evaluated along a linear trajectory labelled by s (in space or time) with a lag τ.[4] Then the PVI time series is

$$\mathrm{PVI}(s; \tau) = \frac{|\Delta\boldsymbol{B}(s, \tau)|}{\sqrt{\langle |\Delta\boldsymbol{B}(s, \tau)|^2 \rangle}}, \tag{5.1}$$

---

[4]The time lag τ is usually selected to correspond to the inertial range of the fluctuations, or in some cases the smallest time lag available in the dataset. For a given analysis, τ is fixed, but results for various values of τ may also be compared.
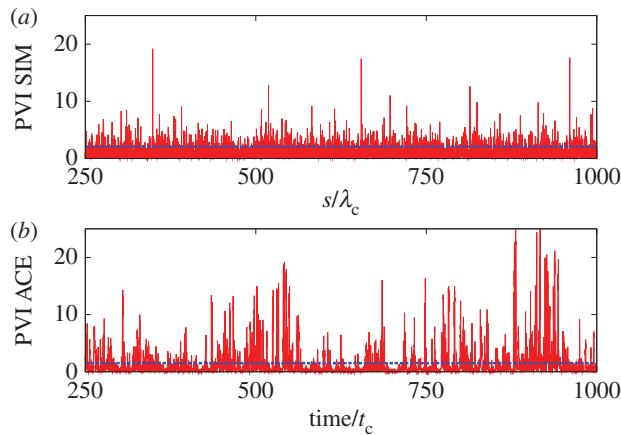
Figure 6. Spatial signal PVI computed from simulation versus distance s/λ_c at a spatial lag $= 0.00625\lambda_c$ (solid thin red line), where λ_c is the correlation scale. (b) Time series PVI (normalized to correlation time t_c) computed from ACE data at a time separation of 4 min. The thick dashed blue lines are the values of the thresholds employed for figure 7. (Online version in colour.)

where the average is over a suitably large *trailing* (i.e. times $< s$) sample computed along the time series. Two sample PVI time series are shown in figure 6, one from a sample of about 750 correlation times of solar wind data and the other from a similar size sample taken from a large two-dimensional MHD turbulence simulation. The simulation is sampled along a linear trajectory analogous to the way that the solar wind data are interpreted using the Taylor hypothesis (spatial lag = time lag × flow speed).

The PVI time series measures the 'spikiness' of the signal relative to its recent past behaviour along the line of observation. In this way, it is a measure of intermittency. It is easy to see that its moments are related to the moments of component increments discussed above that are related to the formal definitions of multi-fractals, etc. PVI turns out to be a useful and easily implemented measure, but it is not unique. Other methods, some based on wavelets [64] such as the local intermittency measure (LIM) [65,66], or distinct techniques such as the phase coherence index the [67] and others, are also useful in quantifying intermittent signals. Our preference for use of PVI is based on its simplicity of implementation, and we are confident that results based on PVI can also be obtained with different methods; for a comparison of PVI and Haar wavelets, see [64].

Upon normalizing the analysis to correlation scales, one may use PVI to compare the distributions of waiting times (or distances) between observed events, defined by selecting a threshold on the PVI value (for a fixed lag and interval of averaging). It is rather remarkable, and, we suggest, significant, that the waiting time distributions in the inertial range of scales are quite comparable in MHD turbulence simulations and in solar wind data (figure 7). As this distribution is a consequence of the nonlinear dynamics in the simulations, the agreement with the solar wind analysis suggests that similar dynamics may cause the statistical distributions of distances between strong discontinuities as measured by PVI.

The distribution of discontinuities is suggestive of some type of boundaries between flux tubes. Furthermore, based on general considerations of anisotropy in MHD [68–70], one would expect the axis of the flux tubes to be roughly aligned with the moderately strong large-scale mean magnetic field of the solar wind. This possibility has been discussed previously, in the context of 'spaghetti models', using different methods for identification [71], and with an interpretation as passive structures originating in the corona. The observation of the boundaries by itself does not answer the question of the origin of the observed structures—whether they are produced *in situ* or are remnants of coronal turbulence. These two are not mutually exclusive, given that the nonlinear age of solar wind turbulence at 1 AU is at most several nonlinear times [72]. It is quite possible then that some observed features can be traced to the wind's coronal origins while others arise *in situ*. A recent study investigated the sharpness of observed discontinuities along
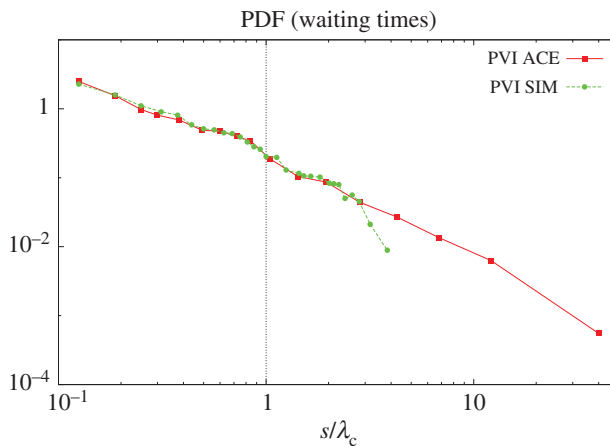
Figure 7. Waiting times (distances) computed from a three-dimensional Hall MHD simulation and from ACE solar wind data, with the coordinate along the time series normalized by the correlation scale. The distributions are very similar and power-law-like in the inertial range. (Adapted from Greco *et al.* [63].) (Online version in colour.)

the Helios orbit, by examining the evolution of the magnetic field PVI distribution, in comparison with similar analysis from MHD simulation [73]. It was found that the solar wind PVI distribution undergoes a subtle but measurable evolution, and that the nature of the evolution is similar to that found in an initial value simulation during the first few nonlinear times. This provides some evidence that part of the evolution of discontinuities or current sheets occurs during solar wind transport to 1 AU.

There is also evidence to be found for cellularization of interplanetary turbulence in solar energetic particle (SEP) data. Prominent in this regard is the phenomenon of SEP dropouts or channelling. Figure 8 shows an example from Mazur *et al.* [74] in which the measured count rates from energetic suprathermal particles sporadically and abruptly turn off, only to suddenly reappear a short time later. One could argue that this is evidence for a flux tube structure, which can topologically trap magnetic field lines [75] as well as particles [76]. Eventually particles can escape these temporary traps but evidently the effect can persist from the corona to 1 AU. More detailed study [77] reveals that flux tubes are likely to have 'trapping boundaries' contained within them that are distinct from the current sheet that may define the outer boundary of the flux tube. A complementary view relates the independence of nearby interplanetary field lines to time dependence of field-line motions at the source [78]. There of course must be a relationship between these ideas as photospheric motions probably set up the original flux tube structure, which maps outwards carried by the solar wind [78]; this connection is distorted by nonlinear effects after a few nonlinear times, but quite possibly it is not erased completely. In any case, it seems clear that flux tubes can act as conduits for transport of SEPs, and this may influence the statistical association of SEP fluxes with PVI events (coherent current structures or discontinuities). Meanwhile there may be leakage of energetic particles from flux tubes owing to particle transport effects, as well as transfer of magnetic field lines from one flux tube to a neighbouring one owing to stochastic component interchange reconnection [79].

A somewhat different but equally compelling view of the cellular structure of turbulence in the solar wind is provided by taking a closer look at the well-known phenomenon of Alfvénic fluctuations [80,81] at 1 AU. The question is whether the distribution of Alfvénic alignment angles in the solar wind is akin to that of active MHD turbulence. As usual, the latter is studied using numerical simulation. An investigation of this nature has been performed [82], using an ensemble of relatively undisturbed turbulence intervals at 1 AU. In one of these, the average normalized cross helicity is $\sigma_c = 2\langle v \cdot b \rangle / \langle v^2 + b^2 \rangle = 0.29$. Then preparing a moderately large Reynolds number incompressible three-dimensional MHD simulation with the same σ_c,
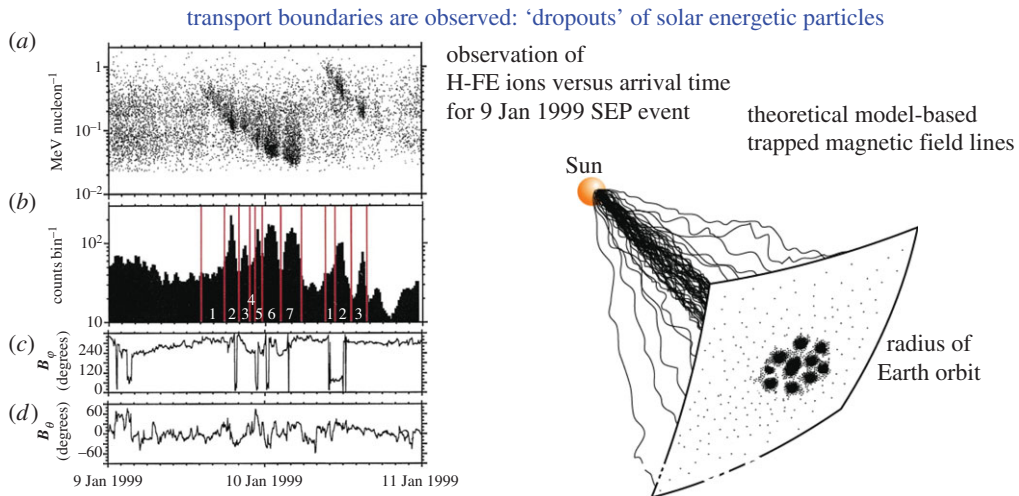
Figure 8. The dropout phenomenon seen in SEP data by Mazur *et al.* [74] is explained by a model based on transient trapping of magnetic field lines within magnetic flux tubes. These act as conduits for transport, delaying diffusion [75]. (Online version in colour.)
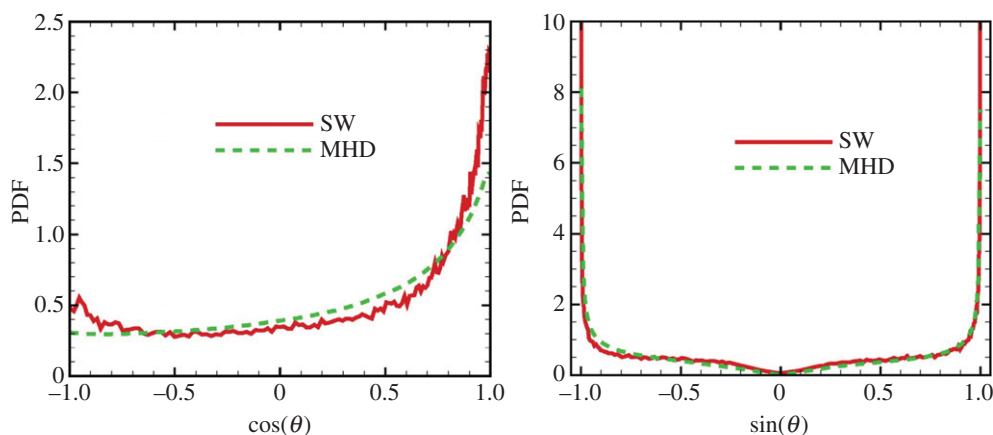

Figure 9. Distributions of $\cos\theta_{vb}$ and $\sin\theta_{vb}$ computed from solar wind (SW) data and from an MHD turbulence simulation initiated with the same dimensionless cross helicity as the solar wind sample. Simulation results are for a time a few nonlinear times from the initial data. The similarity may be viewed as evidence that the spatial patchiness of correlation seen in the simulations, necessarily associated with non-Gaussian distributions, also occurs in the solar wind. (From Osman *et al.* [82].) (Online version in colour.)

one examines the distribution of $\cos\theta_{vb}$ values, where $\theta_{vb}(x)$ is the angle between the velocity and magnetic field fluctuations at each grid point. When the MHD data are of approximately the same age in nonlinear times as the solar wind at 1 AU, one finds that the two distributions of $\cos\theta_{vb}$ are remarkably similar (figure 9). Both populations are peaked at values much more aligned than needed for an average cross helicity of 0.29, while about the same proportion of opposite correlation is found. The latter correspond to subsamples where there is a dominance of 'inward propagating' Elsasser fluctuations. One also finds in the same study that the variety of alignment types exhibited by the cosine distribution actually does occur in patches (not just isolated points), and that this is the case in both the solar wind data and the simulation.

An even broader picture of the patchy alignments associated with relaxation and intermittency is afforded by an analysis of multi-spacecraft *Cluster* data [83]. The four-spacecraft tetrahedral
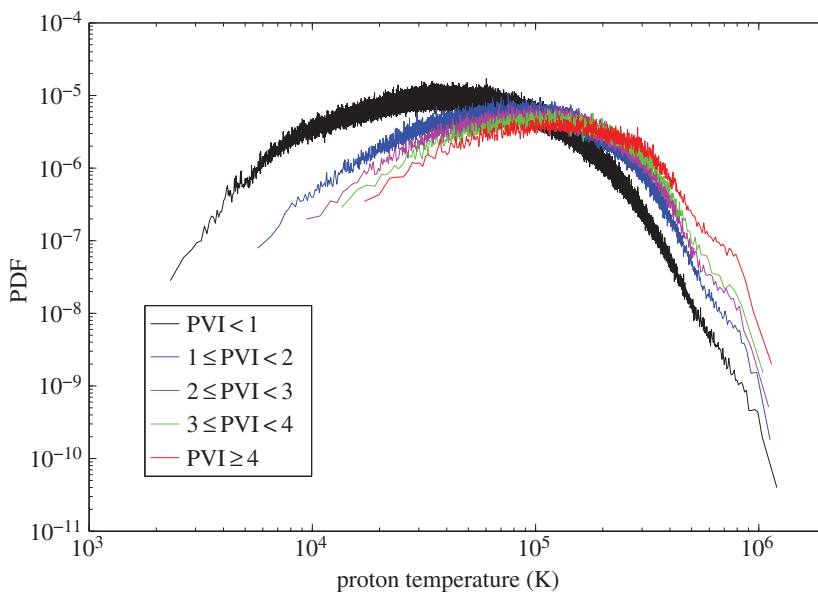
Figure 10. Conditional distributions of proton temperature measured at 1 AU by the ACE spacecraft. The different distributions are for different increasing ranges of PVI value. The higher PVI ranges have distinctly higher temperatures. (From Osman *et al.* [84].) (Online version in colour.)

configuration of *Cluster* permits an approximation to the curl of a measured vector field, so that $\nabla \times \boldsymbol{v}$ and $\nabla \times \boldsymbol{b}$ can be computed and compared with $\boldsymbol{v}$ and $\boldsymbol{b}$. The distributions of the associated alignment cosines, computed for several solar wind intervals [83], are consistent with strong signatures of the force-free correlation, in which the PDF of $\cos\theta_{bj}$, with θ_{bj} the angle between $\boldsymbol{b}$ and its curl, is strongly peaked near ± 1. There is also some evidence of similar peaking in the alignment cosine associated with the Beltrami correlation.

So far we have mainly been concerned with the structure of the observed flux tubes. There is also growing evidence that identified flux tube *boundaries* are sites of heating, as would be expected from considerations analogous to the KRSH, and also of magnetic reconnection, which is expected for some fraction of dynamically active current sheets. When proton temperature distributions are computed conditioned on the value of magnetic field PVI [84] a striking signature is evident: the distributions computed from higher PVI values have temperature distributions that have hotter most probable values, while also displaying stronger high-temperature tails (figure 10). This finding was criticized based on an analysis of nearest neighbour temperatures [85]. However, a more complete analysis of the proton temperatures near PVI events indicates that the average temperature falls off gradually as distance from the identified discontinuities increases [86]. There is a characteristic core of elevated temperature that is about 100 000 km wide and a slower fall-off to distances beyond a correlation scale (approx. 10^6 km). Elevated temperature is not identical to heating, but it may be viewed tentatively as a proxy if heat conduction is not too great. One of the main outstanding problems for a plasma is of course that we do not know the dissipation function (or heat function) from first principles. This is revisited in the next section.

A topic intimately related to both turbulence and intermittency is that of magnetic reconnection [87–90]. In the solar wind, searches for magnetic reconnection have been less successful than in the magnetosphere, in part because the ordered large-scale magnetic field configuration prescribes the regions where the process is likely to be found. In the solar wind studies, instead of searching for the reconnection (diffusion) zones directly, more progress has been achieved based on identification of the Alfvénic exhaust jets that are emitted from an active reconnection site [91,92]. With availability of higher time resolution datasets, larger numbers

of candidate reconnection events have been identified [92]. There has been some controversy as to whether suprathermal particles are associated with some of these events [93,94]. At the same time, if we accept that a turbulence cascade is active in the interplanetary medium, then it seems inescapable that magnetic reconnection in some form must be ongoing. Recently, a PVI-based method was implemented to search for solar wind reconnection sites. The method was tested in the context of MHD simulation [95], where current sheets and reconnection rates can be unambiguously identified by full analysis of the MHD fields. It was found that, for strong events with PVI >6 or 7, it was extremely likely that these would also be located at reconnecting current sheets. In application to the solar wind, the identification of a PVI event with a reconnection site cannot be done in the same way as in the simulations. Instead, a successful identification was defined to be a close coincidence in time of the PVI event with a reconnection event obtained using the Alfvénic exhaust identification strategy. In analogy to the test case, it was found that the data identified by large PVI thresholds was up to 10 000 times more likely to be a reconnection event than a randomly selected point. On the other hand, 90% or more of the large PVI events are not identified exhausts. What is unknown at this time is whether some fraction of these might also be identified as in or near reconnection sites if more inclusive criteria are employed, such as identification of features of the reconnection zone itself instead of just exhausts. From a turbulence perspective, we do expect numerous reconnection sites in the solar wind, but, as seen in simulations, even in two dimensions [89] their features may be complex and rather different in many cases from steady-state laminar Sweet–Parker conditions [96].

This section has attempted a quick review of current progress in understanding the effects of intermittency in the solar wind. It is instructive to conclude by recalling that 35 years ago a prevailing view of the 'turbulence' in the solar wind was that it was a fossil of activity that took place in the lower corona. In this view the fluctuations are described as non-interacting Alfvén waves along with an admixture of classical MHD discontinuities that advect with the wind [80,97]. This perspective stands in contrast to a number of features of interplanetary observations that are consistent with an active turbulence cascade, including, for example, reduction of Alfvénicity, lowering of the Alfvén ratio, development of anisotropy, evolution of the correlation scale [98,99], observed plasma heating [100,101] and the direct measurement of cascade rates [18,102,103]. The recent revival of the so-called spaghetti model of solar wind flux tubes [65,104,105] treats flux tubes and their boundaries, which are static discontinuities, as inert remnants of coronal processes. The interpretation goes so far as to separate the flux tubes and discontinuities from other fluctuations, the latter regarded as 'turbulence'. The various studies alluded to in this section provide a growing body of evidence that the structure that is observed is a consequence of turbulence, either coronal or interplanetary, or both. It also seems difficult not to conclude that coherent structures are involved in the evolution of the solar wind turbulence. Intermittency and structure are therefore an integral part of the cascade, and not a separate inert component. There is still much to be understood about solar wind turbulence and dynamics even at MHD scales. We will now turn to an even more difficult topic, the nature of intermittency at kinetic scales, where the dissipation and heating in plasmas such as the solar wind must occur.

6. Plasma intermittency at kinetic scales

In hydrodynamics, examination of intermittency at scales smaller than the inertial range means characterizing the structures associated with viscous dissipation. MHD intermittency remains less well understood than hydrodynamics but maintains the clarity of well-defined resistive and viscous dissipation functions. An astrophysical plasma such as the solar wind however is only weakly collisional, and numerous plasma processes may influence what is seen at scales smaller than the ion kinetic scales. On the other hand dissipation and heating occupy central roles in understanding the very existence of the solar wind, and therefore these processes are fundamental in a description of the geospace environment and the heliosphere. There are numerous questions that need to be addressed regarding the operative mechanisms and the relative roles of various plasma particle species—electrons, protons, alpha particles, minor species and suprathermal

particles of each type. Intermittency and structure may enter into this environment, but it is expected to be more complex than in the fluid models based on the multiplicity of plasma and electromagnetic variables and the numerous associated length and time scales. Here we briefly review some progress that plasma simulation has been able to make in revealing the complex physics of kinetic plasma intermittency and dissipation.

In some sense one may view the collection of excellent work that has been done on collisionless or weakly collisional magnetic reconnection as a programme of study of kinetic-scale intermittency and coherent structures (e.g. [106–110]). Most of these studies regard reconnection and current sheet dynamics as isolated processes, which for the present purposes is a shortcoming given that coherent structures form and evolve in turbulence as an integral part of the evolution of the entire system. As an example, consider that in most reconnection studies the dominant electric field would typically be the reconnection electric field, which is directly associated with the time rate of change of magnetic flux transferred from one magnetic connectivity to another. However, in a turbulent environment [111], the electric fields associated with the ambient level of turbulence are expected to be much larger than the typical reconnection electric field [89]. This is also apparently true in the solar wind [112]. Therefore, it is not at all certain that coherent current structures in the turbulent environment behave as they do in laminar reconnection simulations. Indeed the break-up of current sheets at high magnetic Reynolds number into multiple reconnection sites, with a proliferation of small flux tubes, seems to indicate that the laminar dynamics of current sheets is difficult to maintain, even in MHD [87,113–117]. For these reasons the study of coherent structures and intermittency in less constrained kinetic plasmas has begun to emerge as an important new direction.

Additional motivation for examining subproton-scale signatures of dissipation and structure comes from the availability of high-resolution solar wind observations. Magnetic field energy spectra extending beyond 100 Hz have enabled exploration and discussion of processes occurring over the full range between proton and electron scales, and beyond [118–121]. Further clues are given by electric field spectra [122], which must be interpreted with some care [123,124]. There are, however, major questions that cannot be addressed only by spectral analysis, such as the relative importance of coherent structures in dissipation and other processes at these scales. Some observational studies [125,126] using very-high-time cadence data have identified small-scale structures that may be associated with dissipation and kinetic-scale reconnection, even down to electron scales. To examine in detail whether such structures may be involved in intermittent dissipation and related kinetic-scale processes, it is necessary to appeal to numerical experiments.

The 2.5-dimensional kinetic hybrid codes are able to capture various aspects of proton (particle) dynamics along with a fluid approximation for electrons. Such codes have shown evolution of proton-scale current sheets in a highly turbulent initial value problem [37] for the case of an out-of-plane guide field. Similar numerical models have also demonstrated stronger Vlasov wave activity [127], when the mean magnetic field lies in the plane of activity.

In another interesting reduced dimensionality approximation, a gyrokinetic simulation model has been able to compute the emergence of current sheets [128,129]. However in this case the intermittency is evidently fairly weak, as the authors were able to show that most of the dissipation could be adequately accounted for by a uniform linear Vlasov heating approximation.

A dramatic demonstration of generation of turbulence and associated formation of structure at kinetic scales was found in the large 2.5-dimensional kinetic particle-in-cell (PIC) model employed by Karimabadi et al. [130]. This model had fully kinetic protons and electrons and was computed on an $8192 \times 16\,384$ grid having a physical resolution of $50d_i \times 100d_i$, measured in ion inertial scales d_i. Initialized with a strong proton shear flow in the plane, and a uniform magnetic field slightly tilted but mainly 'in plane', the system undergoes an interesting evolution from an initial state with no fluid-scale fluctuations at all. Figure 11 provides a brief overview of the turbulence that develops in this undriven initial value problem. Complex structure develops in the electric current density, consisting of interleaved highly dynamic current sheets
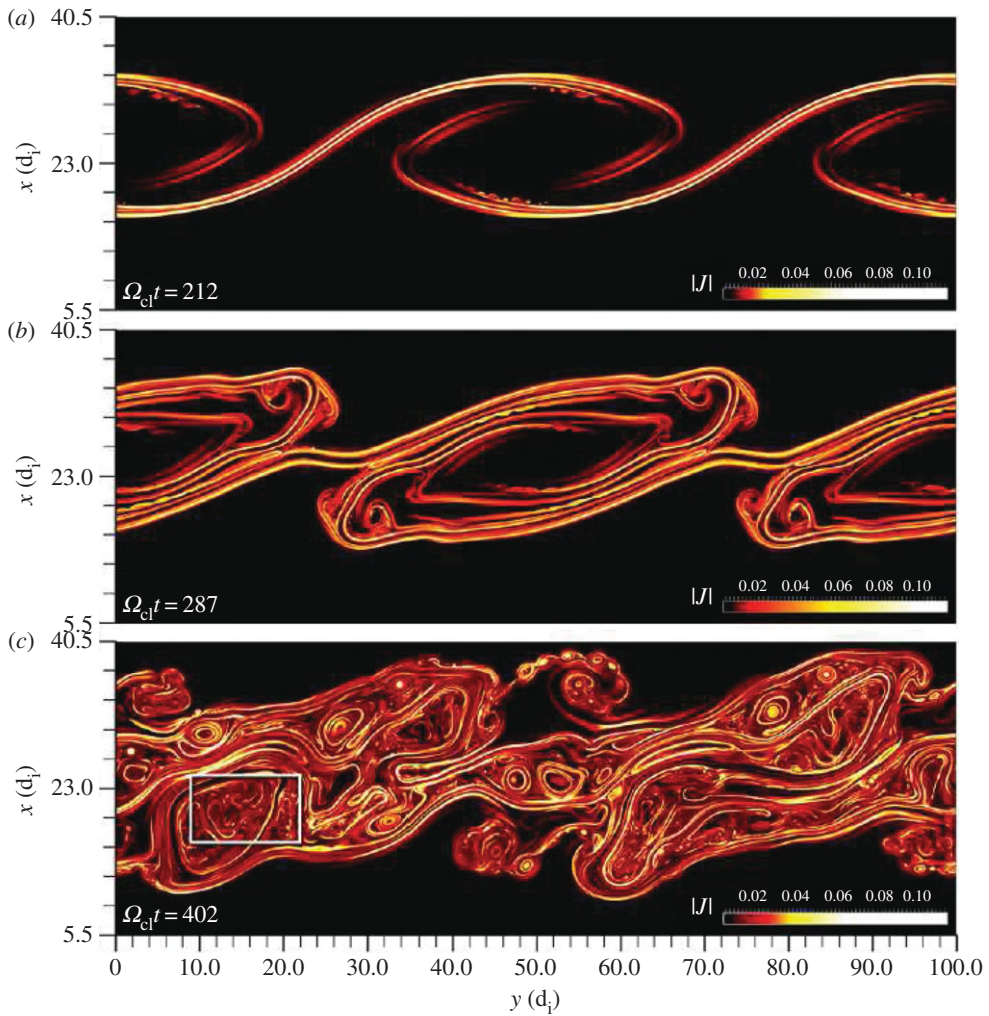
Figure 11. Three images from a large 2.5-dimensional PIC simulation of the development of turbulence starting from a proton shear flow. (From Karimabadi *et al.* [130].) The colour indicates the magnitude of the out-of-plane electric current density where the initial magnetic field is uniform (zero current density). The three phases shown are (*a*) early phase characterized by small perturbations and linear instabilities; (*b*) a transitional phase in which turbulence develops; and (*c*) a strong turbulence phase. It is apparent that small-scale coherent current structures are formed over a range of scales extending fully between proton and electron scales, and also beyond these. (Online version in colour.)

extending at least from several d_i down to scales smaller than the electron inertial scale. (Here the proton/electron mass ratio is 100.)

Using the same simulation, Wan *et al.* [131] analysed the work done by the electromagnetic field on the plasma. Quantitatively this is given by $\boldsymbol{J} \cdot \boldsymbol{E}$, where the electric current density is $\boldsymbol{J}$ and the electric field is $\boldsymbol{E}$. Somewhere buried in this quantity is the work done in producing random motions, i.e. heat, but one must be careful because some of the work included in $\boldsymbol{J} \cdot \boldsymbol{E}$ computed in the laboratory frame is surely not dissipation. For example, it includes work done in producing reversible compressions of the plasma, as well as conversion of magnetic energy into flows, e.g. as in energy release by reconnection. To avoid some of these ambiguities, it is convenient to compute corrections to $\boldsymbol{J} \cdot \boldsymbol{E}$, such as the Zenitani measure [132], which was originally introduced to identify reconnection activity. Other variations include a simple point-by-point evaluation of $\boldsymbol{J} \cdot \boldsymbol{E}$ in the frame of the electron fluid motion, or to compute the work only using the parallel electric field

(parallel to B). Still another variation computes the work using only the current associated with electrons. Wan *et al.* [131] examined all of these, and found in each case that the corresponding work done on the particles is concentrated in sheet-like regions, again spanning a range of scales from $\approx d_i$ to below the electron inertial scales. It was found for example that 70% of the work done on the particles occurs in regions of strong current that occupy less than 7% of the total plasma volume. This falls short of conclusive evidence for intermittent dissipation only owing to the ambiguity of what constitutes effective irreversibility of particle motions.

Massive simulation of magnetic reconnection in three dimensions using the PIC method [109] also reveals the emergence of broadband turbulence. An extensive formal intermittency analysis reveals [133] that the fluctuations in these simulations exhibit non-Gaussian increment distributions, scaling consistent with so-called extended self-similarity and anomalous scaling of higher order moments of the multi-fractal type. Interestingly, all of these properties are also found in fluid-scale hydrodynamic turbulence.

A very basic intermittency property, the scale-dependent kurtosis, can be computed from distinct numerical models to compare and contrast the statistical nature of structure formation under a variety of assumptions. Wu *et al.* [134] recently performed such an analysis, using MHD, Hall MHD and two different 2.5-dimensional PIC codes. The results were also compared with scale-dependent increment kurtosis from several solar wind magnetic field instruments. There is a broad level of agreement that, moving towards smaller scales from within the MHD regime (larger than d_i), one observes an increase in kurtosis. Similarly, within the kinetic scales (smaller than d_i) there is also a general trend towards large kurtosis at smaller scales. However, near or somewhat larger than the proton inertial scale there is a decrease in kurtosis, which may however be due to various systematic and instrumental effects. A physical cause of this has not been established but would be quite interesting and important.[5] Part of the effect is likely also to be due to system size: non-Gaussianity builds up with decreasing scale within a given nonlinear system (see §4), so if a system is small (as in many kinetic codes) its smallest scales struggle to develop the non-Gaussianity associated with nonlinear effects.

Fluctuations in the solar wind kinetic range, and their intermittency properties, have been analysed by a number of other studies as well [136–138] using a variety of approaches. There seems to be a general consensus that the statistics of increments at subproton kinetic scales is non-Gaussian, with some sort of transition in scaling properties seen between the upper MHD inertial range and the kinetic range between proton and electron scales. It is interesting that monofractal, or scale-invariant, behaviour has been reported in several analyses based on *Cluster* data [137, 138], while other analyses argue for strongly increasing scale-dependent kurtosis, and associated departures from self-similarity [136]. The conclusion in the analysis of Wu *et al.* [134] appears to lie somewhere between these, finding a much more rapid increase of kurtosis with decreasing scale in the MHD inertial range, and a more gentle increase in the kinetic range. Interestingly, the Leonardis *et al.* [133] analysis of a single large-scale turbulent reconnection region concludes that the kinetic-scale fluctuations are multi-fractal, and not scale invariant, while analysis of a shear-driven kinetic turbulence [130] appears to favour the conclusion that the small kinetic scales are monofractal. It is encouraging that there is a general consensus that coherent structures are indeed formed in the kinetic-scale cascade. However it is clear that there are some interesting questions regarding kurtosis and other measures at those small scales. Some disagreements may be due to noise (instrumental or numerical) or the presence or absence of waves, or to data interval size and data selection differences. There also may be physics questions, including variability, that are not yet understood. These issues may be settled by improved observations, as well as by running extremely large kinetic codes, perhaps hybrid codes, which we expect will be accomplished in the next few years.

A quite different approach to simulation of turbulence in a collisionless plasma is to compute solutions to the Vlasov–Maxwell equations using Eulerian methods (sometimes called simply

---

[5]Note that a similar feature (local extremum near d_i) is also seen in solar wind observations of the ratio of the quasi-$k_\perp$ energy to the quasi-$k_\parallel$ energy [135]. Podesta [135] suggests this may be due to an enhanced population of waves near $k_\parallel d_i = 1$. It seems likely that such waves would have a different kurtosis from more turbulent fluctuations.
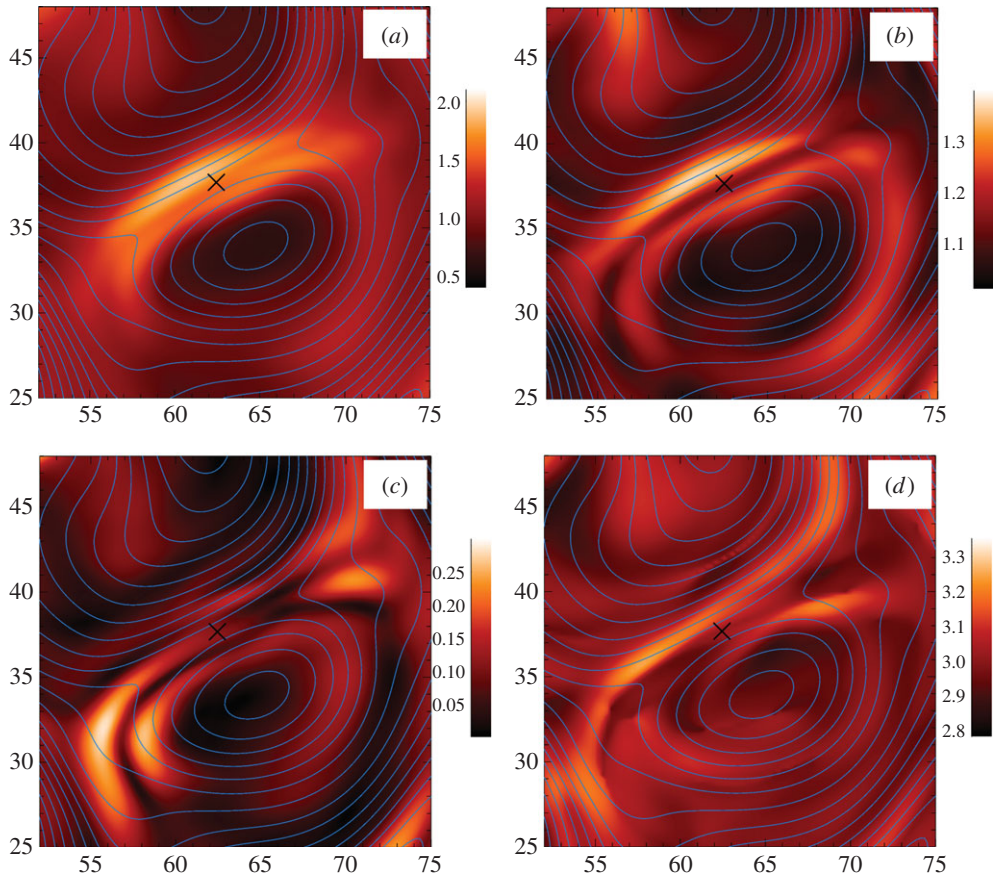
Figure 12. Hybrid Eulerian Vlasov simulation results, showing the concentration of distinctive kinetic features in regions near to current sheets. Colour contours of several quantities in the vicinity of a current sheet (black cross in all panels) with the in-plane magnetic field lines (blue lines): (a) deviation of the proton distribution from an equivalent Maxwellian (in per cent), (b) proton temperature anisotropy $T_\perp/T_\parallel$, (c) proton heat flux and (d) kurtosis of the proton velocities. (From Greco et al. [140].) (Online version in colour.)

Eulerian Vlasov) [95,139]. This method is computationally very expensive but has the distinct advantage of resolving with good fidelity and resolution various properties of the plasma velocity distribution functions. On the other hand, owing to cost, such codes will usually be smaller in units of d_i than tractable PIC codes. Therefore, at present the strength of these codes is in resolving properties of the proton distribution functions, rather than studying scaling or intermittency measures. Hybrid (kinetic protons, fluid electrons) 2.5-dimensional Eulerian Vlasov computations have been able to very well describe coherent current structures near reconnection sites and their statistical association with nearby or co-located regions of kinetic activity such as temperature anisotropies and heat fluxes [95,140,141] (see figure 12 for an illustration). Moreover, results from 2.5-dimensional Eulerian Vlasov codes demonstrate that turbulence can generate distinctive kinetic effects that appear in the $\beta_\parallel, T_\perp/T_\parallel$ plane (parallel plasma beta versus proton temperature anisotropy) [142], and these are similar to observed solar wind features [143–146].

The above results show that in the kinetic regime one finds a great degree of similarity to the fluid and MHD cases: the formation of sheet-like current (or vorticity) structures, concentration of dissipation in coherent structures, non-Gaussianity and anomalous scaling of increment moments. However, it is also clear that new effects enter, such as the distribution of the turbulent

heating into various species [147,148] and a new type of intermittency [95,130] which is the concentration of kinetic features such as anisotropies in coherent structures.

7. Temporal intermittency and very-large-scale structure

Temporal burstiness and intermittency can be due to many types of specific situational causes that would not be subject to a single general theoretical picture. However, in some cases, a nonlinear turbulent system can generate burstiness and long-time correlations owing to simple dynamical processes.

A generic mathematical pathway to '$1/f$' signals in the frequency f domain was described by Montroll & Shlesinger [149] and others. Such signals have very long tails on their two-time correlation functions. This can cause difficulty for prediction, often corresponding to epochal changes in the level of turbulence. This mechanism was invoked to explain the $1/f$ noise that is observed in the solar wind near 1 AU and at high latitudes by *Ulysses* [150–152]. In one version, local parcels of coronal turbulence have a power-law distribution at scales smaller than a correlation length λ_c. But λ_c varies across samples, with a log-normal distribution that has a large variance. Then one can find a range of observed frequencies (or wavenumbers) in which a scale-invariant $1/f$ distribution is observed, as a superposition of the underlying source regions. While this argument has a certain appeal, and could occur in principle owing to scale-invariant reconnection processes in the corona [151], it really reformulates the question to that of explaining the origin of the log-normal distribution of correlation scales. However it is clear that such a process, if it is the cause of the interplanetary signal, would give rise to an episodic bursty-level change of correlation scales and turbulence levels in the solar wind. Interestingly, both correlation scales [153] and energy levels [154] of interplanetary turbulence exhibit log-normal distributions. Random, bursty changes of turbulence amplitude is precisely the situation envisioned by Oboukhov ([4], p. 78), who stated:

> Successive measurements show that, although each measurement is in satisfactory agreement with a $(-\frac{5}{3})$-power-law in a certain range of scales, the intensity of turbulence varies from measurement to measurement, which may be explained by variance of the energy dissipation rate ϵ (the main parameter of the locally isotropic theory). These slow fluctuations of energy dissipation are due to change of the large-scale processes in the observation region, or 'weather' in a general sense. Similar slow macroscopic changes of energy dissipation must be observed at very large Reynolds numbers and they are actually observed in the atmosphere.

This seems to be precisely the type of variability that is expected in the solar wind if observed activity is traceable, at least in part, to source variability. Therefore, an important question is to trace variations of coronal activity to their mechanism of generation.

There has recently been some progress in understanding models that can generate $1/f$ signals, and the associated burstiness and random level changes, from first principles models. One of these systems is the three-dimensional MHD model, including a model of the spherical dynamo. This connection may provide a simple, if not completely detailed, picture of how self-organization at long wavelengths may lead to variability that ultimately drives temporal intermittency. Time dependence of the solar source may therefore ultimately contribute to the observed solar wind variability and low-frequency intermittency.

We direct attention to the result [155] that homogeneous turbulence systems that admit an inverse cascade also display $1/f$ noise and enhanced power at frequencies that are very low compared with the reciprocal of the global nonlinear time scale. This has been found in simulations of two-dimensional hydrodynamics, two-dimensional MHD, and three-dimensional MHD with no mean field. These systems have an inverse cascade and show $1/f$ noise. Conversely, three-dimensional hydrodynamics and non-helical three-dimensional MHD are
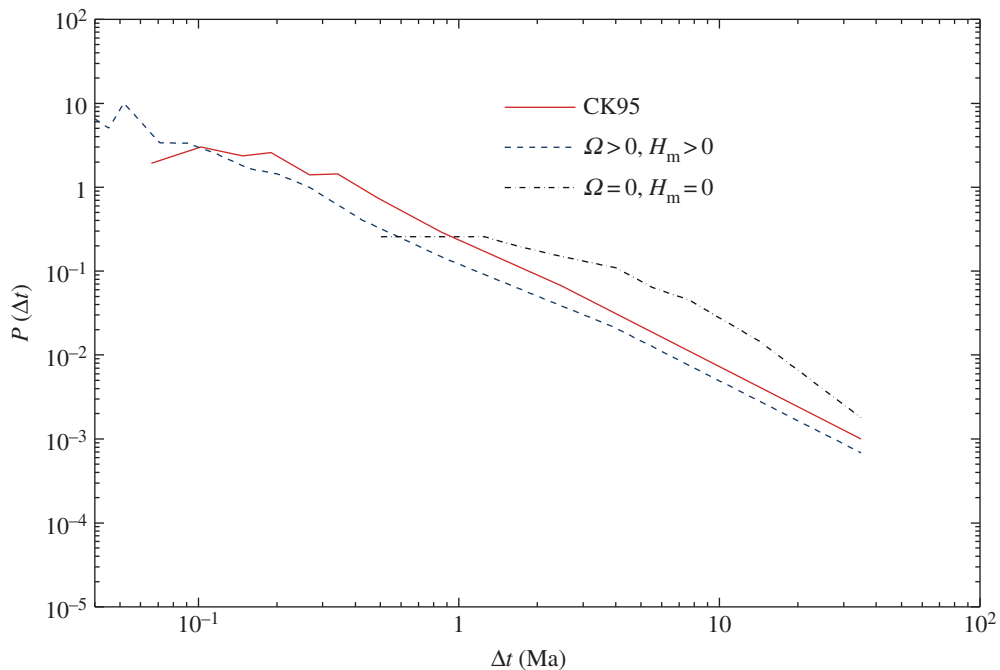
Figure 13. Waiting time distributions for the reversal of the dipole moment in a three-dimensional ideal spherical Galerkin MHD model, compared with the record of geomagnetic reversals. When helicity ($H_m > 0$) and rotation ($\Omega > 0$) are present, the simulation curve exhibits a power-law distribution similar to the geophysical record. When both are absent ($H_m = 0$, $\Omega = 0$), the waiting distribution is very different. (Adapted from Dmitruk *et al.* [160].) (Online version in colour.)

systems that do not show $1/f$ noise and do not have an inverse cascade. Interestingly, when three-dimensional MHD evolves in the presence of a very strong mean magnetic field, the $1/f$ noise reappears. This appears to be because the turbulence becomes very anisotropic and approaches a two-dimensional MHD state. Similarly, rapidly rotating hydrodynamic turbulence also two-dimensionalizes, and begins to recover $1/f$ noise, as found in two-dimensional hydrodynamics.

How do such systems generate time scales that are very long compared with the global nonlinear times? We begin by recalling that scale-to-scale energy transfer in MHD, like hydrodynamics, is dominantly local in the inertial range, consistent with Kolmogorov theory [156,157]. However it turns out that when there is an inverse cascade, or when the system approaches the conditions for inverse cascade, a large fraction of total energy can become tied up in just a few very-large-scale degrees of freedom, which themselves are 'force free' in the generalized sense. Under these conditions the usual Kolmogorov assumption of local transfer is not even approximately correct, and the couplings become very non-local between these energetic modes and the other numerous but low-amplitude modes of the system. This can generate very long and widely distributed characteristic time scales, and thus the $1/f$ noise at frequencies such that $f\tau_{nl} \ll 1$ where τ_{nl} is the global nonlinear time scale. The same style of argument applies equally well to homogeneous MHD [158], rotating hydrodynamics [159] and spherical MHD in a dynamo model [160]. It is of some interest that, in the dynamo model, the $1/f$ noise appears to be directly connected with stochastic reversals of the dipole moment (figure 13). The model remains very primitive even if the basic physics might enter into much more complex solar and heliospheric situations. Further examination of these ideas might eventually link the solar dynamo, solar variability and the statistics of heliospheric properties.
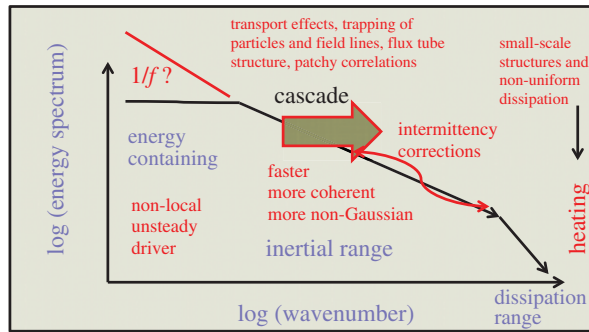
Figure 14. Spectral diagram of plasma turbulence suggesting the cascade and intermittency properties summarized here. Large-scale, non-local effects induce temporal variations, in some cases generate $1/f$ noise, and influence variability at smaller scales, as suggested by Oboukhov [4]. Inertial range cascade is predominantly local in scale but also generates a hierarchy of structures, which in many cases may be viewed as the formation and interaction of a hierarchy of interacting magnetic flux tubes. Significant effects on transport of heat and particles are expected owing to inertial range intermittency. At the smaller scales kinetic processes become important, characteristic coherent small-scale structures (including vortices and current sheets) are formed, secondary instabilities and waves may be in evidence, and ultimately dissipation occurs. (Online version in colour.)

8. Discussion and conclusion

We have presented a brief, informal and probably incomplete review of recent developments in analysis of intermittency and coherent structures associated with turbulence in MHD and plasmas. Rather than emphasizing mathematical formalism, which in any case is not strictly available for the systems of interest, the attempt has been to discuss effects of coherent structures as well as empirical evidence that suggests that their origin is an intrinsic feature of the nonlinear dynamics of turbulence. Using analogy and comparison between numerical simulation and observation, we have attempted to extend the physical interpretation of intermittency effects to features of the solar wind plasma. We may conclude that coherent structures in the inertial range of turbulence have significant potential effects on transport of charged particles, heat, tracers and so on. In short the inertial range is not populated by random-phase coloured noise, but rather by an organized hierarchical cellularized structure of magnetic flux tubes. Indeed there is growing evidence in theory, simulation and observations that rapid relaxation processes sharpen these structures, leading to a state with larger relaxed regions bounded by sharper higher stress near-discontinuities, such as current sheets. 'Dissipation range' intermittency, meaning that which occurs at scales smaller than the inertial range, is connected to these smaller scale structures. Furthermore although we do not know the dissipation function in low-density plasma, there is some evidence accumulating that current sheets and other dissipation range coherent structures are likely to be locations of greatly enhanced dissipation. This is seen in simulation, and indirectly in solar wind observations. We may again briefly summarize the overall perspective we have presented (figure 14).

(a) Low frequencies and very large scales

Structure at very long wavelengths may give rise to temporal intermittency by generation of very long time scales. Systems that exhibit inverse cascade often show a '$1/f$' distribution of noise, which gives rise to random energy-level changes and the associated irregularity in observed statistics. This type of intermittency may be associated with long time behaviour of the dynamo, and therefore may ultimately be implicated in issues of predictability in the photosphere, corona and even the heliosphere. Possible links to issues such as large flares and solar cycle irregularity are topics for future research. At present, it seems likely that irregular distributions of activity on the solar surface should be related to the distribution of solar wind sources, and therefore may be causes of $1/f$ signals seen in the corona and solar wind.

(b) Inertial range intermittency

The well-known turbulent cascade in the solar wind is driven by solar sources and is therefore variable, very much along the lines of the description given by Oboukhov [4]. The variable cascade is highly nonlinear and engages in relaxation processes and the generation of structure. Frequently these take the form of current sheets along borders between adjoining, and sometimes interacting, magnetic flux tubes. The hierarchical structure of flux tubes and current sheets over the several decade range of solar wind turbulence may well be described by an extension of the KRSH which has been discussed in phenomenological terms [20,21,161], but has yet not been fully formulated or tested. On the other hand, it seems evident that the hierarchy of structure found in coronal and solar wind turbulence has important implications for transport phenomena including plasma, suprathermal particles, heat flux and so on. The same structure, viewed dynamically [162], is expected to cause a continual change of magnetic connectivity, which, as far as we are aware, has not been incorporated into many key models of solar wind behaviour.

(c) Beyond the inertial range: intermittent cascade to the kinetic scales

The existing observational perspective on this 'dissipation range intermittency' is very new and not yet very extensive. Much of what is known about kinetic-scale structure emerges from various types of plasma simulation, which is also a rapidly developing field. However many of the recent studies of kinetic dissipation of the turbulent cascade suggest that coherent structures and associated non-uniform dissipation play a very important and possibly dominant role in the termination of the cascade and the effectively irreversible conversion of fluid macroscopic energy into microscopic random motions, i.e. heat. Space missions such as *Magnetospheric Multiscale*, *Solar Orbiter* and *Solar Probe* will greatly clarify the essential heating mechanisms that occur in a low-collisionality plasma subject to turbulence.

References

1. van Dyke M. 1982 *An album of fluid motion*. Stanford, CA: Parabolic Press.
2. Samimy M, Breuer KS, Leal LG, Steen H. 2003 *A gallery of fluid motion*. Cambridge, UK: Cambridge University Press.
3. Novikov EA. 1971 Intermittency and scale similarity in the structure of a turbulent flow. *J. Appl. Math. Mech.* **35**, 231–241. (doi:10.1016/0021-8928(71)90029-3)
4. Oboukhov AM. 1962 Some specific features of atmospheric turbulence. *J. Fluid Mech.* **13**, 77–81. (doi:10.1017/S0022112062000506)
5. Kolmogorov AN. 1962 A refinement of previous hypotheses concerning the local structure of turbulence in a viscous incompressible fluid at high Reynolds number. *J. Fluid Mech.* **13**, 82–85. (doi:10.1017/S0022112062000518)
6. Frisch U. 1995 *Turbulence*. Cambridge, UK: Cambridge University Press.
7. Kolmogorov AN. 1941 Local structure of turbulence in an incompressible viscous fluid at very high Reynolds numbers. *Dokl. Akad. Nauk SSSR* **30**, 301–305. [Reprinted in *Proc. R. Soc. Lond. A* 1991, **434**, 9–13.] (doi:10.1098/rspa.1991.0075)
8. Monin AS, Yaglom AM. 1971 *Statistical fluid mechanics*, vol. 1. Cambridge, MA: MIT Press.
9. Bradshaw P, Cebeci T, Whitelaw J. 1981 *Engineering calculation methods for turbulent flow*. London, UK: Academic Press.
10. Sreenivasan KR, Antonia RA. 1997 The phenomenology of small-scale turbulence. *Annu. Rev. Fluid Mech.* **29**, 435–472. (doi:10.1146/annurev.fluid.29.1.435)
11. She Z, Lévêque E. 1994 Universal scaling laws in fully developed turbulence. *Phys. Rev. Lett.* **72**, 336. (doi:10.1103/PhysRevLett.72.336)
12. Biskamp D. 2003 *Magnetohydrodynamic turbulence*. Cambridge, UK: Cambridge University Press.

13. Verma MK. 2004 Statistical theory of magnetohydrodynamic turbulence: recent results. *Phys. Rep.* **401**, 229–380. (doi:10.1016/j.physrep.2004.07.007)

14. Anselmet F, Gagne Y, Hopfinger EJ. 1984 High-order velocity structure functions in turbulent shear flows. *J. Fluid Mech.* **140**, 63–89. (doi:10.1017/S0022112084000513)

15. Biskamp D, Müller WC. 2000 Scaling properties of three-dimensional isotropic magnetohydrodynamic turbulence. *Phys. Plasmas* **7**, 4889–4900. (doi:10.1063/1.1322562)

16. Sorriso-Valvo L, Carbone V, Veltri P, Consolini G, Bruno R. 1999 Intermittency in the solar wind turbulence through probability distribution functions of fluctuations. *Geophys. Res. Lett.* **26**, 1801–1804. (doi:10.1029/1999GL900270)

17. Politano H, Pouquet A. 1998 von Kármán–Howarth equation for magnetohydrodynamics and its consequences on third-order longitudinal structure and correlation functions. *Phys. Rev. E* **57**, R21–R24. (doi:10.1029/JA095iA12p20673)

18. Coburn JT, Forman MA, Smith CW, Vasquez BJ, Stawarz JE. 2015 Third-moment descriptions of the interplanetary turbulent cascade, intermittency and back transfer. *Phil. Trans. R. Soc. A* **373**, 20140150. (doi:10.1098/rsta.2014.0150)

19. Wan M, Oughton S, Servidio S, Matthaeus WH. 2012 von Kármán self-preservation hypothesis for magnetohydrodynamic turbulence and its consequences for universality. *J. Fluid Mech.* **697**, 296–315. (doi:10.1017/jfm.2012.61)

20. Chandran BDG, Schekochihin AA, Mallet A. 2014 Intermittency and alignment in strong RMHD turbulence. (http://arxiv.org/abs/1403.6354)

21. Merrifield JA, Müller WC, Chapman SC, Dendy RO. 2005 The scaling properties of dissipation in incompressible isotropic three-dimensional magnetohydrodynamic turbulence. *Phys. Plasmas* **12**, 022301. (doi:10.1063/1.1842133)

22. Merrifield JA, Chapman SC, Dendy RO. 2007 Intermittency, dissipation, and scaling in two-dimensional magnetohydrodynamic turbulence. *Phys. Plasmas* **14**, 012301. (doi:10.1063/1.2409528)

23. Wang LP, Chen S, Brasseur JG, Wyngaard JC. 1996 Examination of the hypotheses in the Kolmogorov refined turbulence theory through high-resolution simulations. Part 1. Velocity field. *J. Fluid Mech.* **309**, 113–156. (doi:10.1017/S0022112096001589)

24. Borue V, Orszag SA. 1996 Kolmogorov's refined similarity hypothesis for hyperviscous turbulence. *Phys. Rev. E* **53**, R21–R24. (doi:10.1103/PhysRevE.53.R21)

25. Lee E, Brachet ME, Pouquet A, Mininni PD, Rosenberg D. 2010 Lack of universality in decaying magnetohydrodynamic turbulence. *Phys. Rev. E* **81**, 016318. (doi:10.1103/PhysRevE.81.016318)

26. Oughton S, Wan M, Servidio S, Matthaeus WH. 2013 On the origin of anisotropy in magnetohydrodynamic turbulence: the role of higher-order correlations. *Astrophys. J.* **768**, 10. (doi:10.1088/0004-637X/768/1/10)

27. Milano LJ, Matthaeus WH, Breech B, Smith CW. 2002 One-point statistics of the induced electric field in quasi-normal magnetofluid turbulence. *Phys. Rev. E* **65**, 026310. (doi:10.1103/PhysRevE.65.026310)

28. Rosales C, Meneveau C. 2006 A minimal multiscale Lagrangian map approach to synthesize non-Gaussian turbulent vector fields. *Phys. Fluids* **18**, 075104. (doi:10.1063/1.2227003)

29. Rosales C, Meneveau C. 2008 Anomalous scaling and intermittency in three-dimensional synthetic turbulence. *Phys. Rev. E* **78**, 016313. (doi:10.1103/PhysRevE.78.016313)

30. Subedi P, Chhiber R, Tessein JA, Wan M, Matthaeus WH. 2014 Generating synthetic magnetic field intermittency using a minimal multiscale Lagrangian mapping approach. *Astrophys. J.* **796**, 97. (doi:10.1088/0004-637X/796/2/97)

31. Frisch U, Pouquet A, Sulem PL, Meneguzzi M. 1983 The dynamics of two-dimensional ideal MHD. *J. Mec. Theor. Appl.* **2**, 191–216.

32. Wan M, Oughton S, Servidio S, Matthaeus WH. 2009 Generation of non-Gaussian statistics and coherent structures in ideal MHD. *Phys. Plasmas* **16**, 080703. (doi:10.1063/1.3206949)

33. Zhou Y, Matthaeus WH, Dmitruk P. 2004 Magnetohydrodynamic turbulence and time scales in astrophysical and space plasmas. *Rev. Mod. Phys.* **76**, 1015–1035. (doi:10.1103/RevModPhys.76.1015)

34. Mininni P, Lee E, Norton A, Clyne J. 2008 Flow visualization and field line advection in computational fluid dynamics: application to magnetic fields and turbulent flows. *New J. Phys.* **10**, 125007. (doi:10.1088/1367-2630/10/12/125007)

35. Rappazzo AF, Velli M, Einaudi G. 2010 Shear photospheric forcing and the origin of turbulence in coronal loops. *Astrophys. J.* **722**, 65–78. (doi:10.1088/0004-637X/722/1/65)

36. Greco A, Chuychai P, Matthaeus WH, Servidio S, Dmitruk P. 2008 Intermittent MHD structures and classical discontinuities. *Geophys. Res. Lett.* **35**, L19111. (doi:10.1029/2008GL035454)

37. Parashar TN, Shay MA, Cassak PA, Matthaeus WH. 2009 Kinetic dissipation and anisotropic heating in a turbulent collisionless plasma. *Phys. Plasmas* **16**, 032310. (doi:10.1063/1.3094062)

38. Taylor JB. 1974 Relaxation of toroidal plasma and generation of reverse magnetic fields. *Phys. Rev. Lett.* **33**, 1139–1141. (doi:10.1103/PhysRevLett.33.1139)

39. Montgomery D, Turner L, Vahala G. 1979 Most probable states in magnetohydrodynamics. *J. Plasma Phys.* **21**, 239–251. (doi:10.1017/S0022377800021802)

40. Matthaeus WH, Montgomery D. 1980 Selective decay hypothesis at high mechanical and magnetic Reynolds numbers. *Ann. N. Y. Acad. Sci.* **357**, 203–222. (doi:10.1111/j.1749-6632.1980.tb29687.x)

41. Kraichnan RH. 1967 Inertial ranges in two-dimensional turbulence. *Phys. Fluids* **10**, 1417. (doi:10.1063/1.1762301)

42. Kraichnan RH. 1973 Helical turbulence and absolute equilibrium. *J. Fluid Mech.* **59**, 745–752. (doi:10.1017/S0022112073001837)

43. Frisch U, Pouquet A, Léorat J, Mazure A. 1975 Possibility of an inverse cascade of magnetic helicity in magnetohydrodynamic turbulence. *J. Fluid Mech.* **68**, 769–778. (doi:10.1017/S002211207500122X)

44. Fyfe D, Montgomery D. 1976 High beta turbulence in two-dimensional magnetohydrodynamics. *J. Plasma Phys.* **16**, 181–191. (doi:10.1017/S0022377800020158)

45. Geddes CGR, Kornack TW, Brown MR. 1998 Scaling studies of spheromak formation and equilibrium. *Phys. Plasmas* **5**, 1027–1034. (doi:10.1063/1.872632)

46. Stribling T, Matthaeus WH. 1991 Relaxation processes in a low order three-dimensional magnetohydrodynamics model. *Phys. Fluids B* **3**, 1848–1864. (doi:10.1063/1.859654)

47. Ting AC, Matthaeus WH, Montgomery D. 1986 Turbulent relaxation processes in magnetohydrodynamics. *Phys. Fluids* **29**, 3261–3274. (doi:10.1063/1.865843)

48. Kraichnan RH, Panda R. 1988 Depression of nonlinearity in decaying isotropic turbulence. *Phys. Fluids* **31**, 2395–2397. (doi:10.1063/1.866591)

49. Pelz RB, Yakhot V, Orszag SA, Shtilman L, Levich E. 1985 Velocity-vorticity patterns in turbulent flow. *Phys. Rev. Lett.* **54**, 2505–2508. (doi:10.1103/PhysRevLett.54.2505)

50. Kerr RM. 1987 Histograms of helicity and strain in numerical turbulence. *Phys. Rev. Lett.* **59**, 783–786. (doi:10.1103/PhysRevLett.59.783)

51. Milano LJ, Matthaeus WH, Dmitruk P, Montgomery DC. 2001 Local anisotropy in incompressible magnetohydrodynamic turbulence. *Phys. Plasmas* **8**, 2673–2681. (doi:10.1063/1.1369658)

52. Matthaeus WH, Pouquet A, Mininni PD, Dmitruk P, Breech B. 2008 Rapid alignment of velocity and magnetic field in magnetohydrodynamic turbulence. *Phys. Rev. Lett.* **100**, 085003. (doi:10.1103/PhysRevLett.100.085003)

53. Mason J, Cattaneo F, Boldyrev S. 2006 Dynamic alignment in driven magnetohydrodynamic turbulence. *Phys. Rev. Lett.* **97**, 255002. (doi:10.1103/PhysRevLett.97.255002)

54. Servidio S, Matthaeus WH, Dmitruk P. 2008 Depression of nonlinearity in decaying isotropic MHD turbulence. *Phys. Rev. Lett.* **100**, 095005. (doi:10.1103/PhysRevLett.100.095005)

55. Montgomery DC, Joyce G. 1974 Statistical mechanics of 'negative temperature' states. *Phys. Fluids* **17**, 1139–1145. (doi:10.1063/1.1694856)

56. Montgomery DC, Matthaeus WH, Stribling WT, Martínez D, Oughton S. 1992 Relaxation in two dimensions and the 'sinh-Poisson' equation. *Phys. Fluids A* **4**, 3–6. (doi:10.1063/1.858525)

57. Servidio S, Wan M, Matthaeus WH, Carbone V. 2010 Local relaxation and maximum entropy in two-dimensional turbulence. *Phys. Fluids* **22**, 125107. (doi:10.1063/1.3526760)

58. Biskamp D. 1993 Current sheet profiles in two-dimensional magnetohydrodynamics. *Phys. Fluids B* **5**, 3893. (doi:10.1063/1.860612)

59. Feynman J, Ruzmaikin A. 1994 Distributions of the interplanetary magnetic field revisited. *J. Geophys. Res.* **99**, 17645–17651. (doi:10.1029/94JA01098)

60. Burlaga LF, Ness NF. 1968 Macro- and micro-structure of the interplanetary magnetic field. *Can. J. Phys. Suppl.* **46**, 962–965. (doi:10.1139/p68-394)

61. Tsurutani BT, Smith EJ. 1979 Interplanetary discontinuities: temporal variations and the radial gradient from 1 to 8.5 AU. *J. Geophys. Res.* **84**, 2773–2787. (doi:10.1029/JA084iA06p02773)

62. Neugebauer M. 2006 Comment on the abundances of rotational and tangential discontinuities in the solar wind. *J. Geophys. Res.* **111**, A04103. (doi:10.1029/2005JA011497)

63. Greco A, Matthaeus WH, Servidio S, Chuychai P, Dmitruk P. 2009 Statistical analysis of discontinuities in solar wind ACE data and comparison with intermittent MHD turbulence. *Astrophys. J.* **691**, L111–L114. (doi:10.1088/0004-637X/691/2/L111)

64. Greco A, Perri S. 2014 Identification of high shears and compressive discontinuities in the inner heliosphere. *Astrophys. J.* **784**, 163. (doi:10.1088/0004-637X/784/2/163)

65. Bruno R, Carbone V, Veltri P, Pietropaolo E, Bavassano B. 2001 Identifying intermittency events in the solar wind. *Planet. Space Sci.* **49**, 1201–1210. (doi:10.1016/S0032-0633(01)00061-7)

66. Veltri P, Nigro G, Malara F, Carbone V, Mangeney A. 2005 Intermittency in MHD turbulence and coronal nanoflares modelling. *Nonlin. Process. Geophys.* **12**, 245–255. (doi:10.5194/npg-12-245-2005)

67. Hada T, Koga D, Yamamoto E. 2003 Phase coherence of MHD waves in the solar wind. *Space Sci. Rev.* **107**, 463–466. (doi:10.1023/A:1025506124402)

68. Oughton S, Priest ER, Matthaeus WH. 1994 The influence of a mean magnetic field on three-dimensional MHD turbulence. *J. Fluid Mech.* **280**, 95–117. (doi:10.1017/S0022112094002867)

69. Bieber JW, Wanner W, Matthaeus WH. 1996 Dominant two-dimensional solar wind turbulence with implications for cosmic ray transport. *J. Geophys. Res.* **101**, 2511–2522. (doi:10.1029/95JA02588)

70. Oughton S, Matthaeus WH, Wan M, Osman KT. 2015 Anisotropy in solar wind plasma turbulence. *Phil. Trans. R. Soc. A* **373**, 20140152. (doi:10.1098/rsta.2014.0152)

71. Borovsky JE. 2012 The effect of sudden wind shear on the Earth's magnetosphere: statistics of wind shear events and CCMC simulations of magnetotail disconnections. *J. Geophys. Res.* **117**, A06224. (doi:10.1029/2012JA017623)

72. Matthaeus WH, Smith CW, Oughton S. 1998 Dynamical age of solar wind turbulence in the outer heliosphere. *J. Geophys. Res.* **103**, 6495–6502. (doi:10.1029/97JA03729)

73. Greco A, Matthaeus WH, D'Amicis R, Servidio S, Dmitruk P. 2012 Evidence for nonlinear development of magnetohydrodynamic scale intermittency in the inner heliosphere. *Astrophys. J.* **749**, 105. (doi:10.1088/0004-637X/749/2/105)

74. Mazur JE, Mason GM, Dwyer JR, Giacalone J, Jokipii JR, Stone EC. 2000 Interplanetary magnetic field line mixing deduced from impulsive solar flare particles. *Astrophys. J.* **532**, L79–L82. (doi:10.1086/312561)

75. Ruffolo D, Matthaeus WH, Chuychai P. 2003 Trapping of solar energetic particles by the small-scale topology of solar wind turbulence. *Astrophys. J.* **597**, L169–L172. (doi:10.1086/379847)

76. Tooprakai P, Chuychai P, Minnie J, Ruffolo D, Bieber JW, Matthaeus WH. 2007 Temporary topological trapping and escape of charged particles in a flux tube as a cause of delay in time asymptotic transport. *Geophys. Res. Lett.* **34**, L17105. (doi:10.1029/2007GL030672)

77. Seripienlert A, Ruffolo D, Matthaeus WH, Chuychai P. 2010 Dropouts in solar energetic particles: associated with local trapping boundaries or current sheets? *Astrophys. J.* **711**, 980–989. (doi:10.1088/0004-637X/711/2/980)

78. Giacalone J, Jokipii JR, Matthaeus WH. 2006 Structure of the turbulent interplanetary magnetic field. *Astrophys. J.* **641**, L61–L64. (doi:10.1086/503770)

79. Rappazzo AF, Matthaeus WH, Ruffolo D, Servidio S, Velli M. 2012 Interchange reconnection in a turbulent corona. *Astrophys. J.* **758**, L14. (doi:10.1088/2041-8205/758/1/L14)

80. Belcher JW, Davis Jr L. 1971 Large-amplitude Alfvén waves in the interplanetary medium, 2. *J. Geophys. Res.* **76**, 3534–3563. (doi:10.1029/JA076i016p03534)

81. Roberts DA, Goldstein ML, Klein LW, Matthaeus WH. 1987 Origin and evolution of fluctuations in the solar wind: Helios observations and Helios-Voyager comparisons. *J. Geophys. Res.* **92**, 12023–12035. (doi:10.1029/JA092iA11p12023)

82. Osman KT, Wan M, Matthaeus WH, Breech B, Oughton S. 2011 Directional alignment and non-Gaussian statistics in solar wind turbulence. *Astrophys. J.* **741**, 75. (doi:10.1088/0004-637X/741/2/75)

83. Servidio S, Gurgiolo C, Carbone V, Goldstein ML. 2014 Relaxation processes in solar wind turbulence. *Astrophys. J.* **789**, L44. (doi:10.1088/2041-8205/789/2/L44)

84. Osman KT, Matthaeus WH, Greco A, Servidio S. 2011 Evidence for inhomogeneous heating in the solar wind. *Astrophys. J.* **727**, L11. (doi:10.1088/2041-8205/727/1/L11)

85. Borovsky JE, Denton MH. 2011 No evidence for heating of the solar wind at strong current sheets. *Astrophys. J.* **739**, L61. (doi:10.1088/2041-8205/739/2/L61)

86. Osman KT, Matthaeus WH, Wan M, Rappazzo AF. 2012 Intermittency and local heating in the solar wind. *Phys. Rev. Lett.* **108**, 261102. (doi:10.1103/PhysRevLett.108.261102)

87. Matthaeus WH, Lamkin SL. 1986 Turbulent magnetic reconnection. *Phys. Fluids* **29**, 2513–2534. (doi:10.1063/1.866004)

88. Carbone V, Veltri P, Mangeney A. 1990 Coherent structure formation and magnetic field line reconnection in magnetohydrodynamic turbulence. *Phys. Fluids* **2**, 1487–1496. (doi:10.1063/1.857598)

89. Servidio S, Matthaeus WH, Shay MA, Dmitruk P, Cassak PA, Wan M. 2010 Statistics of magnetic reconnection in two-dimensional magnetohydrodynamic turbulence. *Phys. Plasmas* **17**, 032315. (doi:10.1063/1.3368798)

90. Lazarian A, Eyink G, Vishniac E, Kowal G. 2015 Turbulent reconnection and its implications. *Phil. Trans. R. Soc. A* **373**, 20140144. (doi:10.1098/rsta.2014.0144)

91. Phan TD, Gosling JT, Paschmann G, Pasma C, Drake JF, Oieroset M, Larson D, Lin RP, Davis MS. 2010 The dependence of magnetic reconnection on plasma β and magnetic shear: evidence from solar wind observations. *Astrophys. J.* **719**, L199–L203. (doi:10.1088/2041-8205/719/2/L199)

92. Gosling JT. 2012 Magnetic reconnection in the solar wind. *Space Sci. Rev.* **172**, 187–200. (doi:10.1007/s11214-011-9747-2)

93. Gosling JT, Skoug RM, Haggerty DK, McComas DJ. 2005 Absence of energetic particle effects associated with magnetic reconnection exhausts in the solar wind. *Geophys. Res. Lett.* **32**, L14113. (doi:10.1029/2005GL023357)

94. Wang Y, Wei FS, Feng XS, Zhang SH, Zuo PB, Sun TR. 2010 Energetic electrons associated with magnetic reconnection in the magnetic cloud boundary layer. *Phys. Rev. Lett.* **105**, 195007. (doi:10.1103/PhysRevLett.105.195007)

95. Servidio S, Valentini F, Califano F, Veltri P. 2012 Local kinetic effects in two-dimensional plasma turbulence. *Phys. Rev. Lett.* **108**, 045001. (doi:10.1103/PhysRevLett.108.045001)

96. Parker EN. 1979 *Cosmical magnetic fields: their origin and activity*. Oxford, UK: Oxford Univeristy Press.

97. Barnes A. 1979 Hydromagnetic waves and turbulence in the solar wind. In *Solar system plasma physics*, vol. I (eds EN Parker, CF Kennel, LJ Lanzerotti), p. 251. Amsterdam, The Netherlands: North-Holland.

98. Goldstein ML, Roberts DA, Matthaeus WH. 1995 Magnetohydrodynamic turbulence in the solar wind. *Annu. Rev. Astron. Astrophys.* **33**, 283–325. (doi:10.1146/annurev.aa.33.090195.001435)

99. Tu CY, Marsch E. 1995 MHD structures, waves and turbulence in the solar wind. *Space Sci. Rev.* **73**, 1–210. (doi:10.1007/BF00748891)

100. Coleman PJ. 1968 Turbulence, viscosity, and dissipation in the solar wind plasma. *Astrophys. J.* **153**, 371–388. (doi:10.1086/149674)

101. Matthaeus WH, Zank GP, Smith CW, Oughton S. 1999 Turbulence, spatial transport, and heating of the solar wind. *Phys. Rev. Lett.* **82**, 3444–3447. (doi:10.1103/PhysRevLett.82.3444)

102. MacBride BT, Smith CW, Forman MA. 2008 The turbulent cascade at 1 AU: energy transfer and the third-order scaling for MHD. *Astrophys. J.* **679**, 1644–1660. (doi:10.1086/529575)

103. Sorriso-Valvo L, Marino R, Carbone V, Noullez A, Lepreti F, Veltri P, Bruno R, Bavassano B, Pietropaolo E. 2007 Observation of inertial energy cascade in interplanetary space plasma. *Phys. Rev. Lett.* **99**, 115001. (doi:10.1103/PhysRevLett.99.115001)

104. McCracken KG, Ness NF. 1966 The collimation of cosmic rays by the interplanetary magnetic field. *J. Geophys. Res.* **71**, 3315–3325. (doi:10.1029/JZ071i013p03315)

105. Borovsky JE. 2008 Flux tube texture of the solar wind: strands of the magnetic carpet at 1 AU? *J. Geophys. Res.* **113**, A08110. (doi:10.1029/2007JA012684)

106. Hesse M, Schindler K, Birn J, Kuznetsova M. 1999 The diffusion region in collisionless magnetic reconnection. *Phys. Plasmas* **6**, 1781–1795. (doi:10.1063/1.873436)

107. Shay MA, Drake JF, Rogers BN, Denton RE. 2001 Alfvénic collisionless magnetic reconnection and the Hall term. *J. Geophys. Res.* **106**, 3759–3772. (doi:10.1029/1999JA001007)

108. Ishizawa A, Horiuchi R, Ohtani H. 2004 Two-scale structure of the current layer controlled by meandering motion during steady-state collisionless driven reconnection. *Phys. Plasmas* **11**, 3579–3585. (doi:1063/1.1758718)

109. Daughton W, Roytershteyn V, Karimabadi H, Yin L, Albright BJ, Bergen B, Bowers KJ. 2011 Role of electron physics in the development of turbulent magnetic reconnection in collisionless plasmas. *Nat. Phys.* **7**, 539–542. (doi:10.1038/nphys1965)

110. Roytershteyn V, Karimabadi H, Roberts A. 2015 Generation of magnetic holes in fully kinetic simulations of collisionless turbulence. *Phil. Trans. R. Soc. A* **373**, 20140151. (doi:10.1098/rsta.2014.0151)

111. Dmitruk P, Matthaeus WH. 2006 Structure of the electromagnetic field in three-dimensional Hall magnetohydrodynamic turbulence. *Phys. Plasmas* **13**, 042307. (doi:10.1063/1.2192757)

112. Breech B, Matthaeus WH, Milano LJ, Smith CW. 2003 Probability distributions of the induced electric field of the solar wind. *J. Geophys. Res.* **108**, 1153. (doi:10.1029/2002JA009529)

113. Matthaeus WH, Lamkin SL. 1985 Rapid magnetic reconnection caused by finite amplitude fluctuations. *Phys. Fluids* **28**, 303–307. (doi:10.1063/1.865147)

114. Loureiro NF, Schekochihin AA, Cowley SC. 2007 Instability of current sheets and formation of plasmoid chains. *Phys. Plasmas* **14**, 100703. (doi:10.1063/1.2783986)

115. Bhattacharjee A, Huang YM, Yang H, Rogers B. 2009 Fast reconnection in high-Lundquist-number plasmas due to the plasmoid instability. *Phys. Plasmas* **16**, 112102. (doi:10.1063/1.3264103)

116. Pucci F, Velli M. 2014 Reconnection of quasi-singular current sheets: the 'ideal' tearing mode. *Astrophys. J.* **780**, L19. (doi:10.1088/2041-8205/780/2/L19)

117. Wan M, Matthaeus WH, Servidio S, Oughton S. 2013 Generation of X-points and secondary islands in 2D magnetohydrodynamic turbulence. *Phys. Plasmas* **20**, 042307. (doi:10.1063/1.4802985)

118. Sahraoui F, Goldstein ML, Robert P, Khotyaintsev YV. 2009 Evidence of a cascade and dissipation of solar-wind turbulence at the electron gyroscale. *Phys. Rev. Lett.* **102**, 231102. (doi:10.1103/PhysRevLett.102.231102)

119. Alexandrova O, Saur J, Lacombe C, Mangeney A, Mitchell J, Schwartz SJ, Robert P. 2009 Universality of solar-wind turbulent spectrum from MHD to electron scales. *Phys. Rev. Lett.* **103**, 165003. (doi:10.1103/PhysRevLett.103.165003)

120. Goldstein ML, Wicks RT, Perri S, Sahraoui F. 2015 Kinetic scale turbulence and dissipation in the solar wind: key observational results and future outlook. *Phil. Trans. R. Soc. A* **373**, 20140147. (doi:10.1098/rsta.2014.0147)

121. Riazantseva MO, Budaev VP, Zelenyi LM, Zastenker GN, Pavlos GP, Safrankova J, Nemecek Z, Prech L, Nemec F. 2015 Dynamic properties of small-scale solar wind plasma fluctuations. *Phil. Trans. R. Soc. A* **373**, 20140146. (doi:10.1098/rsta.2014.0146)

122. Bale SD, Kellogg PJ, Mozer FS, Horbury TS, Reme H. 2005 Measurement of the electric fluctuation spectrum of magnetohydrodynamic turbulence. *Phys. Rev. Lett.* **94**, 215002. (doi:10.1103/PhysRevLett.94.215002)

123. Alexandrova O, Chen CHK, Sorriso-Valvo L, Horbury TS, Bale SD. 2013 Solar wind turbulence and the role of ion instabilities. *Space Sci. Rev.* **178**, 101–139. (doi:10.1007/s11214-013-0004-8)

124. Salem CS, Howes GG, Sundkvist D, Bale SD, Chaston CC, Chen CHK, Mozer FS. 2012 Identification of kinetic Alfvén wave turbulence in the solar wind. *Astrophys. J.* **745**, L9. (doi:10.1088/2041-8205/745/1/L9)

125. Sundkvist D, Retino A, Vaivads A, Bale SD. 2007 Dissipation in turbulent plasma due to reconnection in thin current sheets. *Phys. Rev. Lett.* **99**, 025004. (doi:10.1103/PhysRevLett.99.025004)

126. Perri S, Goldstein ML, Dorelli JC, Sahraoui F. 2012 Detection of small-scale structures in the dissipation regime of solar-wind turbulence. *Phys. Rev. Lett.* **109**, 191101. (doi:10.1103/PhysRevLett.109.191101)

127. Verscharen D, Marsch E, Motschmann U, Müller J. 2012 Kinetic cascade beyond magnetohydrodynamics of solar wind turbulence in two-dimensional hybrid simulations. *Phys. Plasmas* **19**, 022305. (doi:10.1063/1.3682960)

128. TenBarge JM, Howes GG, Dorland W. 2013 Collisionless damping at electron scales in solar wind turbulence. *Astrophys. J.* **774**, 139. (doi:10.1088/0004-637X/774/2/139)

129. Howes GG. 2015 A dynamical model of plasma turbulence in the solar wind. *Phil. Trans. R. Soc. A* **373**, 20140145. (doi:10.1098/rsta.2014.0145)

130. Karimabadi H *et al.* 2013 Coherent structures, intermittent turbulence, and dissipation in high-temperature plasmas. *Phys. Plasmas* **20**, 012303. (doi:10.1063/1.4773205)

131. Wan M, Matthaeus WH, Karimabadi H, Roytershteyn V, Shay M, Wu P, Daughton W, Loring B, Chapman SC. 2012 Intermittent dissipation at kinetic scales in collisionless plasma turbulence. *Phys. Rev. Lett.* **109**, 195001. (doi:10.1103/PhysRevLett.109.195001)

132. Zenitani S, Hesse M, Klimas A, Kuznetsova M. 2011 New measure of the dissipation region in collisionless magnetic reconnection. *Phys. Rev. Lett.* **106**, 195003. (doi:10.1103/PhysRevLett.106.195003)

133. Leonardis E, Chapman SC, Daughton W, Roytershteyn V, Karimabadi H. 2013 Identification of intermittent multifractal turbulence in fully kinetic simulations of magnetic reconnection. *Phys. Rev. Lett.* **110**, 205002. (doi:10.1103/PhysRevLett.110.205002)

134. Wu P, Perri S, Osman K, Wan M, Matthaeus WH, Shay MA, Goldstein ML, Karimabadi H, Chapman S. 2013 Intermittent heating in solar wind and kinetic simulations. *Astrophys. J.* **763**, L30. (doi:10.1088/2041-8205/763/2/L30)

135. Podesta JJ. 2009 Dependence of solar-wind power spectra on the direction of the local mean magnetic field. *Astrophys. J.* **698**, 986–999. (doi:10.1088/0004-637X/698/2/986)

136. Alexandrova O, Carbone V, Veltri P, Sorrirso-Valvo L. 2008 Small-scale energy cascade of the solar wind turbulence. *Astrophys. J.* **674**, 1153–1157. (doi:10.1086/524056)

137. Kiyani K, Chapman SC, Khotyaintsev YuV, Dunlop MW, Sahraoui F. 2009 Global scale-invariant dissipation in collisionless plasma turbulence. *Phys. Rev. Lett.* **103**, 075006. (doi:10.1103/PhysRevLett.103.075006)

138. Kiyani K, Chapman SC, Sahraoui F, Hnat B, Fauvarque O, Khotyaintsev YuV. 2009 Enhanced magnetic compressibility and isotropic scale invariance at sub-ion Larmor scales in solar wind turbulence. *Astrophys. J.* **763**, 10. (doi:10.1088/0004-637X/763/1/10)

139. Valentini F, Califano F, Veltri P. 2010 Two-dimensional kinetic turbulence in the solar wind. *Phys. Rev. Lett.* **104**, 205002. (doi:10.1103/PhysRevLett.104.205002)

140. Greco A, Valentini F, Servidio S, Matthaeus WH. 2012 Inhomogeneous kinetic effects related to intermittent magnetic discontinuities. *Phys. Rev. E* **86**, 066405. (doi:10.1103/PhysRevE.86.066405)

141. Valentini F, Servidio S, Perrone D, Califano F, Matthaeus WH, Veltri P. 2014 Hybrid Vlasov–Maxwell simulations of two-dimensional turbulence in plasmas. *Phys. Plasmas* **21**, 082307. (doi:10.1063/1.4893301)

142. Servidio S, Osman KT, Valentini F, Perrone D, Califano F, Chapman S, Matthaeus WH, Veltri P. 2014 Proton kinetic effects in Vlasov and solar wind turbulence. *Astrophys. J.* **781**, L27. (doi:10.1088/2041-8205/781/2/L27)

143. Gary SP. 1993 *Theory of space plasma microinstabilities*. New York, NY: Cambridge University Press.

144. Kasper JC, Lazarus AJ, Gary SP. 2008 Hot solar-wind helium: direct evidence for local heating by Alfvén-Cyclotron dissipation. *Phys. Rev. Lett.* **101**, 261103. (doi:10.1103/PhysRevLett.101.261103)

145. Bale SD, Kasper JC, Howes GG, Quataert E, Salem C, Sundkvist D. 2009 Magnetic fluctuation power near proton temperature anisotropy instability thresholds in the solar wind. *Phys. Rev. Lett.* **103**, 211101. (doi:10.1103/PhysRevLett.103.211101)

146. Osman KT, Matthaeus WH, Kiyani KH, Hnat B, Chapman SC. 2013 Proton kinetic effects and turbulent energy cascade rate in the solar wind. *Phys. Rev. Lett.* **111**, 201101. (doi:10.1103/PhysRevLett.111.201101)

147. Cranmer SR, Matthaeus WH, Breech BA, Kasper JC. 2009 Empirical constraints on proton and electron heating in the fast solar wind. *Astrophys. J.* **702**, 1604–1614. (doi:10.1088/0004-637X/702/2/1604)

148. Wu P, Wan M, Matthaeus WH, Shay MA, Swisdak M. 2013 von Kármán energy decay and heating of protons and electrons in a kinetic turbulent plasma. *Phys. Rev. Lett.* **111**, 121105. (doi:10.1103/PhysRevLett.111.121105)

149. Montroll EW, Shlesinger MF. 1982 On $1/f$ noise and other distributions with long tails. *Proc. Natl Acad. Sci. USA* **79**, 3380–3383. (doi:10.1073/pnas.79.10.3380)

150. Matthaeus WH, Goldstein ML. 1986 Low-frequency $1/f$ noise in the interplanetary magnetic field. *Phys. Rev. Lett.* **57**, 495–498. (doi:10.1103/PhysRevLett.57.495)

151. Mullan DJ. 1990 Sources of the solar wind: what are the smallest-scale structures? *Astron. Astrophys.* **232**, 520–535.

152. Ruzmaikin A, Goldstein BE, Smith EJ, Balogh A. 1996 On the origin of the $1/f$ spectrum of fluctuations in the solar wind. In *Solar wind eight* (eds D Winterhalter, JT Gosling, SR Habbal, WS Kurth, M Neugebauer), p. 382. New York, NY: AIP.

153. Ruiz ME, Dasso S, Matthaeus WH, Weygand JM. 2014 Characterization of the turbulent magnetic integral length in the solar wind: from 0.3 to 5 astronomical units. *Solar Phys.* **289**, 3917–3933. (doi:10.1007/s11207-014-0531-9)

154. Padhye N, Smith CW, Matthaeus WH. 2001 Distribution of magnetic field components in the solar wind plasma. *J. Geophys. Res.* **106**, 18 635–18 650. (doi:10.1029/2000JA000293)

155. Dmitruk P, Mininni PD, Pouquet A, Servidio S, Matthaeus WH. 2011 Emergence of very long time fluctuations and $1/f$ noise in ideal flows. *Phys. Rev. E* **83**, 066318. (doi:10.1103/PhysRevE.83.066318)

156. Verma MK, Ayyer A, Chandra AV. 2005 Energy transfers and locality in magnetohydrodynamic turbulence. *Phys. Plasmas* **12**, 082307. (doi:10.1063/1.1993067)

157. Alexakis A, Mininni PD, Pouquet A. 2005 Shell-to-shell energy transfer in magnetohydrodynamics. I. Steady state turbulence. *Phys. Rev. E* **72**, 046301. (doi:10.1103/PhysRevE.72.046301)

158. Dmitruk P, Matthaeus WH. 2007 Low-frequency $1/f$ fluctuations in hydrodynamic and magnetohydrodynamic turbulence. *Phys. Rev. E* **76**, 036305. (doi:10.1103/PhysRevE.76.036305)

159. Mininni PD, Dmitruk P, Matthaeus WH, Pouquet A. 2011 Large-scale behavior and statistical equilibria in rotating flows. *Phys. Rev. E* **83**, 016309. (doi:10.1103/PhysRevE.83.016309)

160. Dmitruk P, Mininni PD, Pouquet A, Servidio S, Matthaeus WH. 2014 Magnetic field reversals and long-time memory in conducting flows. *Phys. Rev. E* **90**, 043010. (doi:10.1103/PhysRevE.90.043010)

161. Horbury TS, Balogh A, Forsyth RJ, Smith EJ. 1997 ULYSSES observations of intermittent heliospheric turbulence. *Adv. Space Res.* **19**, 847–850. (doi:10.1016/S0273-1177(97)00290-1)

162. Rappazzo AF, Velli M, Einaudi G. 2013 Field lines twisting in a noisy corona: implications for energy storage and release, and initiation of solar eruptions. *Astrophys. J.* **771**, 76. (doi:10.1088/0004-637X/771/2/76)